Dynamics of the transcriptional landscape during human fetal testis and ovary development

Running title: Human fetal gonad transcriptomes

Estelle Lecluze[1], Antoine D. Rolland[1], Panagiotis Filis[2], Bertrand Evrard[1], Sabrina Leverrier-Penna[1,3], Millissia Ben Maamar[1], Isabelle Coiffec[1], Vincent Lavoué[4], Paul A. Fowler[2], Séverine Mazaud-Guittot[1], Bernard Jégou[1], Frédéric Chalmel[1,*]

[1] Univ Rennes, Inserm, EHESP, Irset (Institut de recherche en santé, environnement et travail) - UMR_S 1085, F-35000 Rennes, France.

[2] Institute of Medical Sciences, School of Medicine, Medical Sciences & Nutrition, University of Aberdeen, Foresterhill, Aberdeen, AB25 2ZD, UK.

[3] Univ Poitiers, STIM, CNRS ERL7003, Poitiers Cedex 9, France.

[4] CHU Rennes, Service Gynécologie et Obstétrique, F-35000 Rennes, France.

[*] To whom correspondence should be addressed

Correspondence: frederic.chalmel@inserm.fr.

Abstract

STUDY QUESTION: Which transcriptional program triggers sex differentiation in bipotential gonads and downstream cellular events governing fetal testis and ovary development in humans?

SUMMARY ANSWER: The characterisation of a dynamically-regulated protein-coding and noncoding transcriptional landscape in developing human gonads of both sexes highlights a large number of potential key regulators that show an early sexually dimorphic expression pattern.

WHAT IS KNOWN ALREADY: Gonadal sex differentiation is orchestrated by a sexually dimorphic gene expression program in XX and XY developing fetal gonads. A comprehensive characterisation of its noncoding counterpart offers promising perspectives for deciphering the molecular events underpinning gonad development and for a complete understanding of the aetiology of disorders of sex development in humans.

STUDY DESIGN, SIZE, DURATION: To further investigate the protein-coding and noncoding transcriptional landscape during gonad differentiation, we used RNA-sequencing (RNA-seq) and characterised the RNA content of human fetal testis (N=24) and ovaries (N=24) from 6 to 17 postconceptional week (PCW), a key period in sex determination and gonad development.

PARTICIPANTS/MATERIALS, SETTING, METHODS: First trimester fetuses (6-12 PCW) and second trimester fetuses (13-14 and 17 PCW) were obtained from legally-induced normally-progressing terminations of pregnancy. Total RNA was extracted from whole human fetal gonads and sequenced as paired-end 2x50 base reads. Resulting sequences were mapped to the human genome, allowing for the assembly and quantification of corresponding transcripts.

MAIN RESULTS AND THE ROLE OF CHANCE: This RNA-seq analysis of human fetal testes and ovaries at seven key developmental stages led to the reconstruction of 22,080 transcripts differentially expressed during testicular and/or ovarian development. In addition to 8,935 transcripts

displaying sex-independent differential expression during gonad development, the comparison of testes and ovaries enabled the discrimination of 13,145 transcripts that show a sexually dimorphic expression profile. The latter include 1,479 transcripts differentially expressed as early as 6 PCW, including 39 transcription factors, 40 long noncoding RNAs and 20 novel genes. Despite the use of stringent filtration criteria (expression cut-off of at least 1 fragment per kilobase of exon model per million reads mapped, fold-change of at least 2 and false discovery rate adjusted p-values of less than < 1%) the possibility of assembly artefacts and of false-positive differentially expressed transcripts cannot be fully ruled out.

LARGE SCALE DATA: Raw data files (fastq) and a searchable table (.xlss) containing information on genomic features and expression data for all refined transcripts have been submitted to the NCBI GEO under accession number GSE116278.

LIMITATIONS, REASONS FOR CAUTION: The intrinsic nature of this bulk analysis, i.e. the sequencing of transcripts from whole gonads, does not allow direct identification of the cellular origin(s) of the transcripts characterised. Potential cellular dilution effects (e.g. as a result of distinct proliferation rates in XX and XY gonads) may account for a few of the expression profiles identified as being sexually dimorphic. Finally, transcriptome alterations that would result from exposure to pre-abortive drugs cannot be completely excluded. Although we demonstrated the high quality of the sorted cell populations used for experimental validations using quantitative RT-PCR, it cannot be totally excluded that some germline expression may correspond to cell contamination by, for example, macrophages.

WIDER IMPLICATIONS OF THE FINDINGS: For the first time, this study has led to the identification of a thousand of protein-coding and noncoding candidate genes showing an early, sexually dimorphic, expression pattern that have not previously been associated with sex differentiation. Collectively, these results increase our understanding of gonad development in

humans, and contribute significantly to the identification of new candidate genes involved in fetal gonad differentiation. The results also provide a unique resource that may improve our understanding of the fetal origin of testicular and ovarian dysgenesis syndromes, including cryptorchidism and testicular cancers.

STUDY FUNDING/COMPETING INTEREST(S): This work was supported by the French National Institute of Health and Medical Research (Inserm), the University of Rennes 1, the French School of Public Health (EHESP), the Swiss National Science Foundation [SNF n° CRS115_171007 to B.J.], the French National Research Agency [ANR n° 16-CE14-0017-02 and n°18-CE14-0038-02 to F.C], the Medical Research Council [MR/L010011/1 to PAF] and the European Community's Seventh Framework Programme (FP7/2007-2013) [under grant agreement no 212885 to PAF]] and from the European Union's Horizon 2020 Research and Innovation Programme [under grant agreement no 825100 to PAF and SMG]. There are no competing interests related to this study.

Keywords: Human gonad development; fetal testis; fetal ovary; sex differentiation; disorders of sex development; transcriptional profiling; novel unannotated transcripts; long noncoding RNAs; bulk RNA-sequencing; proteomics informed by transcriptomics.

Introduction

Mammalian ovary and testis development is a unique process compared to other organ development, both developing from a bipotential organ which commits to a different fate following gonadal sex determination and ending up as entirely different organs. This decisive turning point guides the gonad toward one of the two developmental pathways, both including specific cell type development and proliferation. Proper differentiation of these cell lineages determines the reproductive health of the future being. In humans, the gonadal primordium arises from the thickening of the coelomic epithelium at the surface of the mesonephros around 4th postconceptional week (PCW, corresponding to 6 weeks of gestation/amenorrhea), and contains several precursor cell types, notably precursors of supporting and steroidogenic cell lineages, as well as primordial germ cells (PGC) (Wilhelm *et al.*, 2013). The expression of the Y-linked transcription factor sex-determining region Y (SRY) during the 6th PCW in supporting cell precursors of the genital ridge triggers the expression of the SRY-box transcription factor 9 (SOX9) transcription factor which subsequently promotes a highly orchestrated gene expression program (Koopman *et al.*, 1991; Vidal *et al.*, 2001; Sekido and Lovell-Badge, 2008; Li *et al.*, 2014; Rahmoun *et al.*, 2017). These molecular events activate the commitment of Sertoli cells, leading to testis cord formation, the appearance of a fetal Leydig cell from 7 PCW onwards, and production of male hormones (androgens, insulin-like 3 protein and anti-Müllerian hormone) that are essential for embryo masculinization. In the absence of SRY the R-spondin 1 (RSPO1)/Wnt family member 4 (WNT4)/β-catenin pathway and forkhead box L2 (FOXL2) induce another complex cascade of transcriptional events, giving rise to fetal ovaries marked by the differentiation of pre-granulosa cells and the commitment of germ cells into meiosis from 10 PCW onwards (Vainio *et al.*, 1999; Schmidt, 2004; Uda *et al.*, 2004; Ottolenghi *et al.*, 2007; Chassot *et al.*, 2008; Liu *et al.*, 2009; Le Bouffant *et al.*, 2010; Childs *et al.*, 2011). To ensure the appropriate commitment to a given fate, the sex-specific pathways antagonize each other to repress the alternative fate (Kim and Capel, 2006;

Chang *et al.*, 2008; Maatouk *et al.*, 2008; Wilhelm *et al.*, 2009; Kashimada *et al.*, 2011; Jameson *et al.*, 2012a; Greenfield, 2015; Bagheri-Fam *et al.*, 2017). Sex differentiation therefore stems from a critical moment triggering a complex transcriptional landscape that governs gonad specification and organogenesis. Both male and female expression programs are highly dynamic and complex, but many blank areas remain in the map of our understanding, thus preventing full understanding of most disorders of sex development (DSDs) (Eggers *et al.*, 2016). In particular, the noncoding counterpart of the transcriptome is likely to play critical roles in the physiology and the pathophysiology of the human developing gonads (Wu *et al.*, 2016).

Many dedicated studies have investigated *in situ* the gonadal expression pattern of specific human genes and/or proteins known to play important roles in sex determination or gonad development (Hanley *et al.*, 1999, 2000; de Santa Barbara *et al.*, 2001; Ostrer *et al.*, 2007; Mamsen *et al.*, 2017). In addition, several valuable genome-wide expression studies have used microarray technology to analyze whole fetal gonads (Small *et al.*, 2005; Fowler *et al.*, 2009; Houmard *et al.*, 2009; Rolland *et al.*, 2011; Munger *et al.*, 2013; del Valle *et al.*, 2017; Mamsen *et al.*, 2017) or isolated fetal gonadal cell populations (Nef *et al.*, 2005; Beverdam and Koopman, 2006; Bouma *et al.*, 2007, 2010) in several mammalian species, including human. Recently single-cell transcriptomic analyses of thousands of cells have opened up a new window onto gonadal cell lineages during fetal life (Guo *et al.*, 2015, 2017; Li *et al.*, 2017; Stévant *et al.*, 2018, 2019). Although the latest technologies hold great potential for further investigations, they are currently limited in their ability to study alternative splicing, decipher the noncoding expression program or discover novel genes (Haque *et al.*, 2017). Alternatively, “bulk” RNA-sequencing (RNA-seq) can be used to circumvent these issues (Gkountela *et al.*, 2015). Several landmark studies have performed RNA-seq in the mouse to investigate the transcriptome of the fetal Leydig cells (McClelland *et al.*, 2015; Inoue *et al.*, 2016), the regulome of the key gonadal transcription factor SOX9 (Rahmoun *et al.*, 2017), and the transcriptome of the developing fetal testes and ovaries

at key developmental stages (Zhao *et al.*, 2018). Despite the limited availability of normal fetal human gonads, RNA-seq analyses of gonad development in humans represent a very precious resource for our understanding.

In the present study, we performed a strand-specific, ribo-depleted RNA sequencing approach to unravel the protein-coding and noncoding transcriptional landscape of human developing fetal testes and ovaries from 6 to 17 PCW. Selected time-points were chosen to encompass the time window from early transcription of the SRY gene in the male to differentiation and primary sex-specific control of the cell lineages in both gonads. This analysis allowed us to identify a complex sexually and non-sexually dimorphic expression program driving gonad development, with a focus on non-coding genes as well as new unannotated genes that had not previously been described. In particular we have highlighted a core set of transcripts showing a sex-biased expression after the onset of SRY expression within the whole gonad during the 6^{th} PCW that likely plays a critical role in fetal gonad differentiation, and potentially for sex determination in humans. Our study significantly expands knowledge of human gonadogenesis and provides a rich source of data for geneticists and clinicians working in the field of DSDs.

Materials and Methods

Ethical considerations and sample collection

First trimester fetuses

Human fetuses (8-14 GW) were obtained from legally-induced normally-progressing terminations of pregnancy performed in Rennes University Hospital. Tissues were collected with women's written informedconsent, in accordance with the legal procedure agreed by the National Agency for Biomedical research (#PFS09-011) and the approval of the Local ethics committee of Rennes Hospital (# 11-48). The termination of pregnancy was induced using a standard combined mifepristone and misoprostol protocol, followed by aspiration. Gestational age was determined by ultrasound, and further confirmed by measurement of foot length for mathematical estimation of fetal development (Evtouchenko *et al.*, 1996; O'Shaughnessy *et al.*, 2019). The gonads were recovered and dissected free of mesonephros in ice-cold phosphate-buffered saline (PBS) using a binocular microscope (Olympus SZX7, Lille, France). The sex of the gonad was determined by morphological criteria, except for fetuses younger than 7 PCW, for which a PCR was performed on genomic DNA using primers specific for SRY (ACAGTAAAGGCAACGTCCAG; ATCTGCGGGAAGCAAACTGC) (Friel *et al.*, 2002) as well as for amelogenin X-linked (AMELX) and amelogenin Y-linked (AMELY) (CTGATGGTTGGCCTCAAGCCTGTG; GTGATGGTTGGCCTCAAGCCTGTG) (Akane *et al.*, 1992).

Second trimester fetuses

Human fetuses (13-14 and 17 PCW) were obtained from pregnant women after legally induced abortions at the Aberdeen Pregnancy Counselling Service. The collection of fetal material was approved by the National Health Service (NHS) Grampian Research Ethics Committees (REC

04/S0802/21). In all cases, women seeking elective terminations of pregnancy were recruited with full written, informed consent by nurses working independently of the study at the Aberdeen Pregnancy Counselling Service. Maternal data and medications used were recorded. Only fetuses from normally progressing pregnancies (determined at ultrasound scan prior to termination) from women over 16 years of age were collected following termination induced by a standard combined mifepristone and misoprostol protocol, as detailed previously (O'Shaughnessy *et al.*, 2007; Fowler *et al.*, 2008). Fetuses were transported to the laboratory within 30 min of delivery, weighed, sexed and the crown-rump length recorded. Fetal tissues were snap-frozen in liquid nitrogen and stored at -80°C.

RNA extraction, library construction and RNA-sequencing

Total RNA was extracted from human fetal gonads using the RNeasy mini Kit (Qiagen, Hilden, Germany), quantified using a NanoDrop™ 8000 spectrophotometer (Thermo Fisher Scientific, Waltham, MA, USA) and quality controlled using a 2100 Electrophoresis Bioanalyzer (Agilent Technologies, Santa Clara, CA, USA). Only RNA extracts with a high quality RNA integrity number (average value = 9.8 - ranging from 8.6 to 10) were included. Libraries suitable for strand-specific high throughput DNA sequencing were then constructed, essentially as previously described (Jégou *et al.*, 2017; Rolland *et al.*, 2019) using "TruSeq Stranded Total RNA with Ribo-Zero Gold Prep Kit" (catalog # RS-122-2301, Illumina Inc., San Diego, CA, USA). The libraries were finally loaded in the flow cell at 7 pM concentration and clusters were generated in the Cbot and sequenced in the Illumina Hiseq 2500 as paired-end 2x50 base reads following Illumina's instructions. Image analysis and base calling were performed using RTA 1.17.20 and CASAVA 1.8.2.

Read mapping, transcript assembly and quantification with the Tuxedo suite

Assembly of a unique set of human reference transcripts

Ensembl (Yates *et al.*, 2016) and RefSeq (Pruitt *et al.*, 2014; Brown *et al.*, 2015) transcript annotations (GTF format) of human genome (release hg19) were downloaded from the UCSC (Speir *et al.*, 2016) in June 2015, and were merged with Cuffcompare (Pollier *et al.*, 2013). This non-redundant annotation was then used as the human reference transcripts (HRT) as previously published (Chalmel *et al.*, 2014). A non-redundant dataset of human splice junctions (HSJ) was also extracted from alignments of human transcripts and expressed sequence tags on the human genome as provided by UCSC.

Read mapping

Reads from each individual sample were aligned to the hg19 release of the human genome with TopHat2 (version 2.0.12) (Trapnell *et al.*, 2012) using previously published approaches (Pauli *et al.*, 2012; Trapnell *et al.*, 2012; Chalmel *et al.*, 2014; Zimmermann *et al.*, 2015). Briefly, TopHat2 program was first run for each fastq file, using HRT and HSJ datasets to improve read mapping. Exonic junction outputs were then merged and added to the HSJ set. TopHat2 was next run a second time using the new HSJ dataset to produce a final alignment file (BAM format) for each. Finally, BAM files corresponding to the same experimental condition (fetal testes or ovaries, at a given time-point) were merged and sorted with the Samtools suite (version 2.19.0) (Li *et al.*, 2009).

Transcriptome assembly and quantification

The Cufflinks suite (version 2.2.1, default settings) (Pollier *et al.*, 2013) was used to assemble transcript fragments (or transfrags) for each experimental condition based on merged BAM files. Resulting assembled transcripts were further merged into a non-redundant set of transfrags which were further compared to the HRT dataset with the Cuffcompare program. Finally, Cuffquant was used to estimate abundance of each transcript in each individual sample as fragments per kilobase of exon

model per million reads mapped (FPKM), and the normalization of the expression values across samples was performed by Cuffnorm.

Refinement of assembled transcripts

A four-step strategy was used to filter out dubious transcripts as previously described (Prensner *et al.*, 2011; Chalmel *et al.*, 2014) (Fig. S1). First, based on the Cuffcompare comparison, we only selected transfrags defined as complete match ('='), potentially novel isoform ('j'), falling entirely within a reference intron ('i') or an intergenic region ('u'), or showing exonic overlap with reference on the opposite strand ('x'). Next, assembled transcripts of less than 200 nucleotides or that were undetectable (<1 FPKM) were discarded. Finally, all transfrags that were annotated as either novel isoforms or novel genes (class codes "j", "i", "u" or "x") and that did not harbor at least two exons (multi-exonic) were filtered out.

Principal component analysis

Principal component analysis (PCA) was performed based on the expression values of refined transcripts with the FactoMineR package to graphically evaluate the distribution of sequenced samples (Lê *et al.*, 2008).

Coding potential analysis of assembled transcripts

DNA sequences of the refined transcripts were extracted with TopHat's gffread tool. As recommended in (Chocu *et al.*, 2014; Zimmermann *et al.*, 2015), the protein-coding potential of each transcript was estimated with an empirical integrative approach based on four predictive tools: Coding-Potential Assessment Tool (CPAT, coding probability > 0.364) (Wang *et al.*, 2013), HMMER (E-value < 10-4) (Finn *et al.*, 2011), Coding Potential Calculator (CPC, class "coding") (Kong *et al.*, 2007) and txCdsPredict (score >800) (Kuhn *et al.*, 2013). Finally, we considered assembled transcripts to likely

encode for proteins if their nucleic sequences were considered as protein-coding by at least two predictive tools.

Proteomics informed by transcriptomics strategy

As previously published in (Chocu *et al.*, 2014; Rolland *et al.*, 2019), we made use of a Proteomics Informed by Transcriptomics (PIT) approach (Evans *et al.*, 2012) to provide evidence at the protein level for assembled transcripts. First, we assembled a customized non-redundant protein database by merging the UniProt (Pundir *et al.*, 2015) and the Ensembl (Yates *et al.*, 2016)(downloaded 2015/10) proteome databases together with the set of predicted proteins derived from the assembled transcripts. Briefly, the refined transcript sequences were translated into the three-first open reading frames with the EMBOSS's Transeq program (Rice *et al.*, 2000) and only the amino acid sequences of at least 20 residues were selected.

We next made use of the human fetal gonad MS/MS proteomics datasets available from the Human Proteome Map (Kim *et al.*, 2014). First, 131 raw data files (corresponding to three fetal ovary samples and two fetal testis samples) were downloaded from the PRIDE database (accession number PXD000561) (Vizcaíno *et al.*, 2016) and converted into mgf format with ProteoWizard (Adusumilli and Mallick, 2017). Subsequent analyses were performed with SearchGUI (Vaudel *et al.*, 2011) (version 3.2.20) and PeptideShaker (Vaudel *et al.*, 2015)(version 1.16.8). A concatenated target/decoy database was created from the enriched reference proteome with SearchGUI. Cross-peptide identification was then performed with X!Tandem, Open Mass Spectrometry Search Algorithm (OMSSA), and MSGF+ tools, with these following parameters: precursor ion tolerance units set at 10 ppm; fragment tolerance set at 0.05 Da; carbamidomethylation of cysteine defined as a fixed modification; oxidation of methionine and acetylation of protein N-term defined as a variable

261 modification; only tryptic peptides with up to two missed cleavages; and minimum peptide length set
262 to six amino acids. All peptides with at least one validated peptide spectrum match (PSM) and a
263 confidence score greater than 80% with PeptideShaker, were kept for further analyses. Finally, only
264 identifications with a false discovery rate (FDR) <1% were selected.

265

266 Statistical transcript filtration

267 The set of sexually dimorphic transcripts (SDTs) was defined by filtering transfrags that exhibited a
268 $\geqslant$ 2-fold difference between the male and female gonads (using median expression values of sample
269 replicates) in at least one of the seven developmental stages. A Linear Models for Microarray Data
270 (LIMMA) statistical test was then used to identify transcripts displaying significant changes between
271 male and female gonads (F-value adjusted with a FDR $\leqslant$ 5%) (Smyth, 2004). Among SDTs, those
272 showing a differential expression as early as 6 PCW were designated as the set of early SDTs (or early-
273 SDTs). In addition, the set of developmental regulated transcripts (DRTs) were also selected by
274 isolating transfrags that exhibited a $\geqslant$ 2-fold difference between two developmental stages during
275 either male or female gonad development. Similar to the selection of SDTs, a F-value adjusted with a
276 FDR $\leqslant$ 5% was then used to identify candidates showing significant variations across developmental
277 stages. Finally, the difference between the sets of DRTs and SDTs allowed us to discriminate non-
278 sexually dimorphic transcripts (NSDTs) corresponding to the set of transfrags showing a
279 developmentally regulated expression pattern across fetal gonad development, but no significant
280 differential expression between male and female gonads.

281

Cluster and functional analyses

The resulting SDTs and NSDTs were then clustered into fourteen (named P1-14) and six (Q1-6) expression patterns with the unsupervised hierarchical clustering on principle components (HCPC) algorithm, respectively (Lê *et al.*, 2008). These clusters were then ordered according to peak expression levels across developmental stages in testes first and then ovaries. Gene Ontology (GO) term enrichments were estimated with the Fisher exact probability, using a Gaussian hypergeometric test implemented in the Annotation Mappin Expression and Network suite (AMEN) (Chalmel and Primig, 2008). A GO term was considered significantly associated with a given expression pattern if the FDR-corrected P value was $\leqslant$5% and the number of genes bearing this annotation was $\geqslant$5.

Transcription factors and their related target genes

To get an insight into potentially important regulators that might be involved in early human gonad development or sex determination, transcriptional factors and their targets were extracted from public databases, the Transcriptional Regulatory Relationships Unraveled by Sentence-based Text mining database (TRRUST) (Han *et al.*, 2015) and Transcription Factor encyclopedia (Yusuf *et al.*, 2012).

FACS sorting and quantitative PCR validation

Single cell dissociation and cell sorting

Single cell suspensions were obtained from gonads by a standard enzymatic and mechanic digestion procedure. Gonads were cut into small pieces and digested in 0.25% Trypsin-0.02% EDTA (#T4049, Sigma-Aldrich) and 0.05 mg/ml DNase (#DN25, Sigma-Aldrich, Missouri, USA) for 10 min at 37 °C. Trypsin digestion was stopped by adding 10% fetal bovine serum in M199 media and samples were

centrifuged at 350 g for 5 min at 37°C. Dispersed cells were resuspended in PBS and counted on a Malassez hemocytometer after labeling of dead cells with Trypan blue. For testes, a plasma membrane labelling of cord cells was performed using a mouse FITC-conjugated anti-human epithelial antigen (clone Ber EP4; Dako # F0860, diluted 1:100) associated with a labelling of germ cells with a mouse R-Phycoerythrin-coupled anti-human KIT proto-oncogene, receptor tyrosine kinase (KIT/CD117) (clone 104D2, BioLegend, San Diego, CA, USA, # 313204, diluted 1:100) for 30 min at room temperature. For ovaries, germ cells were labeled with the mouse R-Phycoerythrin-coupled anti-human KIT/CD117 as described above. Cells were sorted by a flow cytometer cell sorter FACSAriaII (BD Biosciences, New Jersey, USA) equipped with Diva software. Cells were collected in PBS, centrifuged at 500g for 45 min at 4°C and pelleted cells were stored at -80°C until RNA extraction.

Quantitative RT-PCR

RNA was extracted from cell pellets with PicoPure RNA Isolation Kit (Thermo Fisher Scientific) according to manufacturer's instructions. Total RNAs (100 ng) were reverse transcribed with iScript cDNA synthesis kit (Biorad, Hercules, CA, USA) and quantitative PCR was performed using the iTaq© universal SYBR green supermix (Biorad) according to manufacturer's instructions in a Cfx384 OneTouch Real-Time PCR system (Biorad). The following amplification program was used: an initial denaturation of 3 min at 95°C, 40 cycles of 10 sec denaturation at 95°C and 30 sec at 62°C for annealing and extension. Dissociation curves were produced using a thermal melting profile performed after the last PCR cycle. Primer pairs flanking introns were designed in order to avoid amplification of contaminating genomic DNA whenever possible and they were aligned onto human RefSeq transcripts using primer-BLAST to check for their specificity. Furthermore, only those primers that produced a single peak during the melting curve step (i.e. with peak temperature variance of no more than 0.5°C) were considered and their efficiency was evaluated using serial dilutions of cDNA templates (Table

328 I). Ribosomal protein lateral stalk subunit P0 (RPLP0) and ribosomal protein S20 (RPS20) mRNA,
329 used as internal controls for normalization purposes, were initially validated in human adult testis
330 gonad (Svingen *et al.*, 2014) and further used for human fetal gonads (Jørgensen *et al.*, 2018). Results
331 were calculated with Bio-Rad CFX Manager 3.1 using the ΔΔCT method as n-fold differences in target
332 gene expression, relative to the reference gene and calibrator sample, which comprises an equal
333 mixture of all the tested samples for a given organ.

334

335 Immunohistochemistry and immunofluorescence

336 Upon collection, additional gonads (seven testes and five ovaries) were fixed either in Bouins fluid
337 fixative or paraformaldehyde 4% (w/v) for 1 to 2 hours, embedded in paraffin using standard
338 procedures and cut into 5 µm-thick sections. After dewaxing and rehydration, slides were treated for
339 antigen retrieval with pre-heated 10 mM citrate buffer, pH 6.0 at 80°C for 40 min before cooling at
340 room temperature . Sections were blocked for 1 h at room temperature with 4% bovine serum albumin
341 in PBS before the overnight incubation at 4°C with the primary antibody diluted in Dako antibody
342 diluent (Dako Cytomation, Trappes, France). Antibodies and conditions are described in Table II.
343 Secondary antibodies were goat anti-rabbit biotinylated antibody (E0432, Dako, diluted 1:500); or
344 rabbit anti-mouse biotinylated antibody (E0464, Dako, diluted 1:500). Sections were developed with
345 streptavidin-horseradish peroxidase (Vectastain ABC kit, Vector Laboratories, Burlingame, CA, USA)
346 and 3,3'-diaminobenzidine tetrahydrochloride (Vector Laboratories Inc.) and counterstained with
347 hematoxylin. Stained sections were examined and photographed under light microscopy (Olympus
348 BX51). For cryosectioning, additional paraformaldehyde-fixed gonads were cryopreserved in PBS-
349 sucrose 20%, embedded in NEG50TM (Allan-Richard Scientific, Thermo Fisher Scientific) and cut in
350 8 µm-thick sections. Thawed sections were treated for antigen retrieval with citrate buffer, as

351 described, when necessary (for WT1 transcription factor, WT1; neurexin 3, NRXN3; contactin 1,
352 CNTN1; and lin-28 homolog A, LIN28), rinsed in PBS and incubated overnight at 4°C with primary
353 antibody. Rinsed sections were incubated with the ad hoc fluorescent secondary antibodies (1:500).
354 The second primary antibody was subsequently incubated overnight at 4°C followed by the
355 corresponding secondary antibody. Secondary antibodies were either 488 or 594 Alexa Fluor
356 conjugated antibodies made in chicken for rabbit- and mouse-hosted primary antibodies, and in donkey
357 for Contactin 1 (CNTN1) primary antibody (Invitrogen). Sections were mounted in prolong Gold anti-
358 fade reagent with DAPI (Invitrogen, Carlsbad, CA, USA; Thermo Fisher Scientific). Slides were
359 examined and photographed with an AxioImager microscope equipped with an AxioCam MRc5
360 camera and the ZEN software (Zeiss, Le Pecq, France).

361

Results

Expression profiling of fetal gonads identifies more than 300 new genes in the human genome

To investigate the expression program governing gonad differentiation in humans, we performed a RNA-seq analysis on fetal testes *(n*=24) and ovaries (*n*=24), covering seven developmental stages from 6 to 17 PCW (i.e. from 8 to 19 gestational weeks) (Fig. 1A). Following read mapping and transcript reconstruction (Supplementary Table SI), a stringent refinement strategy selected a "high-confidence" set of 35,194 transcripts expressed in human fetal gonads (Supplementary Fig. S1). A PCA of these expression data provided a first hint on the biological relevance of our dataset: The first three components indeed appeared strongly correlated with the developmental stage (dimensions 1 and 3) and the genetic sex (dimension 2) of samples (19.7% and 15.3% of variance, respectively) (Fig. 1B and C). A hierarchical clustering based on the 35 first PCA dimensions explaining 90% of the total variance of the data further confirms the reliable distribution of the samples according to the sex and the developmental stage (Fig. 1D).

The comparison of reconstructed transcripts with RefSeq and Ensembl reference annotations identified known (13,673; 38.9%) and novel (18,718; 53.2%) isoforms of annotated protein-coding genes as well as known (529, 1.5%) and novel (680, 1.9%) isoforms of annotated long noncoding RNAs (lncRNAs). Importantly this comparison also identified 318 novel unannotated transcripts (NUTs) corresponding to new intronic (81, 0.2%), intergenic (164, 0.5%) or antisense (73, 0.2%) as yet uncharacterized genes in the human genome. The comparison of genomic and expression features highlighted significant differences between mRNAs, lncRNAs and NUTs (Supplementary Fig. S2). As expected, lncRNAs are expressed at lower levels than mRNAs, are more specifically expressed during single stages of development, and have lower sequence conservation, length, number of exons and GC content. Interestingly, this "non-coding" trend is exacerbated by NUTs, as they have a lower abundance,

conservation, length, number of exons and GC content as well as a more restricted expression than lncRNAs and mRNAs (Supplementary Fig. S2).

We next combined results from a coding potential analysis and from a proteomics informed by transcriptomics approach (PIT) (Evans *et al.*, 2012) to characterize the protein-encoding potential of novel isoforms and loci identified above. As expected, 98.5% of mRNAs (known and novel isoforms) displayed a high protein-encoding potential, and 56% of them were supported at the protein level thanks to at least one identified peptide (Fig. 1E). On the other hand, only 48.1% of lncRNAs (known and novel isoforms) were predicted to have a high protein-encoding potential (PEP), and as little as 8.5% were identified during the PIT analysis, usually through a single peptide identification (Fig. 1E). When NUTs were finally evaluated, they mostly displayed features similar to lncRNAs: 76.1% of them were predicted to have a low protein-encoding potential while only 0.4% were confirmed at the protein level (Fig. 1E). Besides, 94 lncRNAs (including 53 with two or more peptides identified) and one NUT were both predicted to have a high protein-encoding potential and demonstrated at the protein level.

Transcriptome dynamics during human gonad development define sexually and non-sexually dimorphic expression programs

We next focused on genes with dynamic expression patterns during gonad development. Several steps of statistical filtration led to the selection of 13,145 transcripts (7,633 genes) that were differentially-expressed between testes and ovaries (called SDT), most of which (10,521 transcripts, 6,587 genes) were also developmentally-regulated (Fig. 1F). Notably, 8,935 transcripts (5,961 genes) were differentially-expressed during gonad development but did not show significant difference between sexes (NSDT).

We further classified SDT into 14 clusters (termed P1-P14) according to their preferential expression pattern (Fig. 2A and B). Patterns P1-P7 include transcripts showing peak expression in fetal testes at 6 to 7 PCW (P1; *SRY*; doublesex and mab-3 related transcription factor 1,*DMRT1*), at 7 PCW (P2; *SOX9*, desert hedgehog signalling molecule, *DHH*; inhibin subunit beta B, *INHBB*), at 9 to 12 PCW (P4; cytochrome P450 family 11 subfamily A member 1, *CYP11A1*; cytochrome P450 family 17 subfamily A member 1, *CYP17A1*; steroidogenic acture regulatory protein, *STAR*; luteinizing hormone/choriogonadotropin receptor, *LHCGR*; insulin like 3, *INSL3*), at 13 to 17 PCW (P6; actin alpha 2, *ACTA2;* prostaglandin D2 synthase, *PTGDS*) or with a broader expression pattern throughout testis development (P3; nuclear receptor subfamily 5 group A member 1, *NR5A1*; nuclear receptor subfamily 0 group B member 1, *NR0B1;* and P5; WT1 transcription factor, *WT1;* claudin 11 *CLDN11*). Similarly, transcripts belonging to patterns P8-P14 are preferentially expressed in fetal ovaries and display peak expression at 7 PCW (P8; *RPSO1*, anti-Mullerian hormone receptor type 2, *AMHR2*; nanog homeobox, *NANOG*), at 7-9 PCW (P9; POU class 5 homeobox 1, *POU5F1*; developmental pluripotency associated 2 and 4, *DPPA2*/*4;* lin-29 homolog A and B, *LIN28A*/*B*), at 12 PCW (P11; *FOXL2*, deleted in azoospermia like, *DAZL;* piwi like RNA-mediated gene silencing 2, *PIWIL2*), at 13-14 PCW (P12; MET proto-oncogene, receptor tyrosine kinase, *MET;* delta like canonical Notch ligand 4, *DLL4;* X inactive specific transcript, *XIST;* vascular endothelial growth factor A, *VEGFA*), at 17 PCW (P13; meiotic double-stranded break formation protein 1, *MEI1;* meiosis specific with OB-fold, *MEIOB;* SPO11 initiator of meiotic double stranded breaks, *SPO11;* synaptonemal complex protein 1 to 3, *SYCP1-3;* and P14; folliculogenesis specific bHLH transcription factor, *FIGLA;* NOBOX oogenesis homeobox, *NOBOX;* spermatogenesis and oogenesis specific basic helix-loop-helix 1, *SOHLH1*) or with a broader expression throughout ovarian development (P10; DNA meiotic recombines 1, *DMC1;* empty spiracles homeobox 2, *EMX2;* lymphoid enhancer binding factor 1 *LEF1;* Wnt family member 2B, *WNT2B*). We also evaluated the functional relevance of expression

patterns by a GO term enrichment analysis (Fig. 2C). Several broad biological processes related to organogenesis and/or cell differentiation were enriched in various testis-associated (P1, P2, P5, P6) and ovary-associated (P8) patterns. More precisely, expression pattern P4 was found to be enriched in genes involved in steroidogenesis while several processes associated with meiosis and female germ cell development were found to be enriched in P13 and P14, which is consistent with the differentiation and development of Leydig cells in fetal testes from 7 PCW onwards and with the commitment of ovarian germ cells into meiosis from 12 PCW onwards, respectively. Finally, we investigated the distribution of RNA biotypes and found that lncRNAs and NUTs were significantly enriched in expression patterns P12 to P14 (Fig. 2D).

The 8,935 NSDTs were also classified according to peak expression into six expression patterns (termed Q1-Q6) and include transcripts expressed at early stages of gonad differentiation (6-7 PCW; Q1 and Q2; including *WT1*, GATA binding protein 4, *GATA4*), following sexual differentiation (7-9 PCW; Q3 and Q4; *DMRT1*, SRY-box transcription factor 8, *SOX8*) or at later stages of gonad development (12-17 PCW; Q5 and Q6; nuclear receptor subfamily 6 group A member 1, *NR6A1*) (Fig. 3A-C). Finally, when investigating the distribution of RNA biotypes within co-expression groups, we found that lncRNAs and NUTs were enriched in expression patterns Q1 and Q6 (Fig. 3D). While these transcripts are also likely to include factors with important roles during gonadal differentiation and development, they were not further investigated in this study. All data, however, are available through the ReproGenomics Viewer (RGV) genome browser (http://rgv.genouest.org/) (Darde *et al.*, 2015, 2019) and are also available as a searchable table (.xlss) containing information on genomic features and expression data for all refined transcripts (submitted to the NCBI GEO under accession number GSE116278).

454 A complex transcriptional program governing early gonadal differentiation

455 In order to highlight new candidate genes that could be involved in early gonadal differentiation, we
456 focused our analysis on 1,479 SDTs showing a significant differential expression in fetal gonads as
457 early as 6 PCW (Supplementary Fig. S3). Most of these early-SDTs (61.7%) logically belong to early
458 expression patterns P1, P2, P8 and P9. This set of genes is composed of important actors including
459 *SRY* (P1), *SOX9*, *DHH*, patched 1 (*PTCH1*) and cytochrome P450, family 26 subfamily b polypeptide
460 1 (*CYP26B1*) (P2), LIM homeobox 9 (*LHX9*) (P6), activin A receptor type 1B (*ACVR1B*) (P8), *AMHR2*
461 (P9) or *FOXL2* (P11) which demonstrates the relevance of this filtration for selecting important factors
462 in sex differentiation (Supplementary Fig. S3B and S3C). In addition to well-known transcription
463 factors, such as SRY, SOX9, LHX9, or FOXL2, 174 early SDTs correspond to 131 genes encoding
464 transcriptional regulators that should also play a critical role in the establishment of this complex
465 sexually dimorphic expression program (Supplementary Table SII). Although the proportion of early-
466 SDTs in the distinct expression patterns P1-P14 according to their coding status are generally similar
467 to those of SDT (Supplementary Fig. S3D), it is important to note that this set of candidates includes
468 40 lncRNAs and 20 NUTs which may be involved in early steps of gonad differentiation.

469

470 Distinct cellular expression patterns of newly identified genes involved in human sex determination

471

472 To investigate further the cellular origin of selected candidates, we performed immunohistochemistry
473 experiments as well as quantitative PCR (qPCR) on FACS-sorted cells. The successful enrichment of
474 Sertoli cells (hEpA+/KIT-), germ cells (KIT+) and interstitial cells (hEpA-/KIT-) from 6–7 PCW testes
475 was notably validated by the expression of *SOX9*, KIT proto-oncogene, receptor tyrosine kinase (*KIT*)
476 and nuclear receptor subfamily 2 group F member 2 (*NR2F2*), respectively (Supplementary Fig. S4A-

C), while that of germ cells (KIT+) and somatic cells (KIT-) from 6–8 PCW and 10–12 PCW ovaries was confirmed by the high expression levels of *KIT, FOXL2* or *NR2F2*, respectively (Supplementary Fig. S4D-F). We first investigated genes that display expression profiles similar to that of *SRY* (P1; high expression and clear sexual dimorphism in 6 PCW testes), such as Wnt ligand secretion mediator (*WLS*), C-X-C motif chemokine ligand 14 (*CXCL14*) and C-C motif chemokine receptor 1 (*CCR1*) (Fig. 4A). While *WLS* was mainly expressed in Sertoli cells it was also substantially expressed in interstitial cells, whereas *CXCL14* was only expressed in Sertoli cells (Fig. 4A). In contrast, the expression of *CCR1* was mainly detected in germ cells. We also analysed genes with an expression profile similar to *SOX9* (P2; clear sexual dimorphism and peak of expression in 7 PCW testes), such as EPH receptor B1 (*EPHB1*), fetal and adult testis expressed 1 (*FATE1*), MAGE family member B1 (*MAGEB1*), erb-b2 receptor tyrosine kinase 3 (*ERBB3*), Cbp/p300 interacting transactivator with Glu/Asp rich carboxy-terminal domain 1 (*CITED1*) and a NUT antisense to CITED1 (TCONS_00249587) (Fig. 4B). We found that *EPHB1*, *FATE1*, *MAGEB1* and *ERBB3* were indeed expressed in Sertoli cells and to a lesser extent in interstitial cells, while SRY-box transcription factor 10 (*SOX10)* was expressed at similar levels in Sertoli cells and interstitial cells (Fig. 4B). Interestingly, we found that both *CITED1* and its potential antisense RNA were specifically and simultaneously expressed in Sertoli cells. Consistently with qPCR results, SOX10, EPHB1, MAGEB1, and FATE1 proteins were indeed all found in cord cells at the histological level, but exhibited varying ratios of expression in Sertoli and germ cells (Fig. 4C). For instance, SOX9 was expressed only in Sertoli cells, whereas MAGEB1 was clearly expressed in germ cells as well.

We also investigated the cell distribution of genes preferentially expressed in ovary (P8-P9) (Fig. 5A-D). First, several of them show a higher differential expression as early as 6 PCW, and were preferentially expressed in somatic cells, including neurexin 3 (*NRXN3*), contactin 1 (*CNTN1*) and SET nuclear proto-oncogene (*SET*), or specifically in somatic cells such as the NUT

501 *TCONS_00153406* (Fig. 5A). In agreement, immunolabeling showed NRXN3 protein in the nucleus
502 of cells surrounding KIT+ germ cells, with a pattern very similar to that of WT1 (Fig. 5D).
503 Interestingly, CNTN1 protein was found in a subset of epithelial cells surrounding LIN28+ germ cells
504 in 6 PCW ovaries, or in ovarian cords adjacent to the mesonephric-gonadal junction (Fig. 5D) but not
505 in the surface epithelium. Several genes show higher levels of differential expression at later stages in
506 gonad development (Fig. 5B-C). Some of those genes, such as neuropeptide Y (*NPY*), SRY-box
507 transcription factor 4 (*SOX4*) and the novel transcript *TCONS_00224470*, were preferentially
508 expressed in somatic cells, as was *RSPO1* (Fig. 5B). In contrast, others displayed patterns typical of
509 germline-associated expression patterns, including *POU5F1* (a well-known germ cell marker) and
510 three NUTs, *TCONS_00113718*, *TCONS_00055038* and *TCONS_00042565*, which were highly
511 expressed in female germ cells from 7 to 12 PCW (Fig. 5C).

Discussion

Unravelling the molecular sequence of events involved in gonadogenesis and sex determination is essential in order to understand DSDs. Although a significant number of studies have already examined the sexually dimorphic expression program driving gonad development in animal models (Beverdam and Koopman, 2006), its characterization remains elusive in humans. Three studies have investigated the transcriptome of the developing gonads from 5.7 to 10 PCW (Mamsen et al., 2017; del Valle et al., 2017) and of ovarian primordial follicle formation from 13 to 18 PCW (Fowler *et al.*, 2009) in humans. However, they were based on microarray technologies, thus restricting the gene set studied and limiting the characterization of non-coding transcripts and the identification of new genes. Our study is among the first to capitalize on the power of the "bulk" RNA-seq technology to perform an in-depth characterization of the dynamic transcriptional landscape of whole human fetal gonads, from early differentiation (i.e. 6 PCW) up to Leydig cell transition in the testis and primary follicle formation in the ovary (i.e. 17 PCW), at both the protein-coding and non-coding levels. In particular our results identify transcriptional regulators, lncRNAs and novel genes (NUTs) that show an early sexually dimorphic expression pattern and could therefore play important regulatory roles from sex determination onwards. Nevertheless, as in any model, including animals that are sacrificed with anesthesia or CO_2 or in the case of spontaneous abortions where the development of the embryo or foetus can be disturbed, it should be borne in mind that there is a small chance that some transcriptional alterations might result from exposure to pre-abortive drugs. Collectively this work constitutes a rich resource for the community by providing new information regarding the early molecular events that could be involved in both normal sex differentiation and DSDs.

Our study confirms and complements previous findings accumulated in humans and other species (Nef *et al.*, 2005; Beverdam and Koopman, 2006; Jameson *et al.*, 2012b; Zhao *et al.*, 2018; Planells *et al.*, 2019). For instance our dataset validates the onset of *SRY* transcription prior to 6 PCW (detected at 5.5

PCW in (Mamsen *et al.*, 2017)) but also demonstrates the over-expression of *SOX9* in the testis as early as 6 PCW (previously reported at only 6.8 PCW in (Mamsen *et al.*, 2017)), which may reflect the higher sensitivity of RNA-seq as compared to microarrays (Mantione *et al.*, 2014). Altogether our transcriptional profiling allowed us to identify over 33,000 transcripts expressed in human developing fetal gonads, including mRNAs and lncRNAs as well as unknown genes. Although our analysis was mostly focused on SDTs, a set of almost 9,000 transcripts showing similar expression profiles in testes and ovaries (NSDTs) was also identified despite major cell composition differences between the two gonad types, especially at later developmental stages. These transcripts therefore represent valuable information on critical molecular factors underlying or required for the development of both XX and XY gonads, including for instance WT1 and its multiple isoforms required at different stages (Hastie, 2017).

We then focused our analysis on 1,479 SDTs showing sexual dimorphism as early as 6 PCW, including more than 1,000 candidate genes that have not previously been associated with sex differentiation. It is noteworthy that most of these early dimorphic profiles are likely to result from true differential transcriptional regulation rather than from dilution effects, as the cell composition of XX and XY fetal gonads at this stage remains highly analogous. To further highlight new promising candidates that might be involved in the regulation of this complex expression program we next focused on the 131 genes encoding transcription factors and showing an early SDT pattern (Supplementary Table SII). Among them, the cAMP responsive element modulator (CREM), a well-known regulator of gene expression programming of post-meiotic germ cells in the adult testis (Hogeveen and Sassone-Corsi, 2006), is preferentially expressed in XY gonads at 6 PCW. We also found that one of its target genes, the tachykinin precursor 1 (*TAC1*) (Qian *et al.*, 2001), is over-expressed in the fetal ovary at this early developmental stage suggesting that CREM might negatively regulate TAC1 in the human fetal testis. While its role during sex determination remains unknown, TAC1 encodes several neuropeptides

belonging to the tachykinin family that are critical for many biological processes (Dehlin and Levick, 2014; Sun and Bhatia, 2014; Sorby-Adams *et al.*, 2017). GLI family zing finger 1 (*GLI1)* is also an interesting candidate as it is preferentially expressed in the fetal testis as early as 6 PCW (Mamsen *et al.*, 2017) and encodes a transcription factor known to regulate the expression of the secreted frizzled related protein 1 (SFRP1) (Kim *et al.*, 2010). Since SFRP1 is critical for fetal testis development in the mouse (Warr *et al.*, 2009), acting through its suppression of Wnt signalling (Kim *et al.*, 2010), this could suggest a potential important role for both *GLI1* and *SFRP1* during sex differentiation in humans.

Mamsen and collaborators deduced from their microarray experiment that the onset of steroidogenesis in male gonads occurred at 7.5 PCW (Mamsen *et al.*, 2017). We also consistently found that the expression of genes involved in steroidogenesis increased drastically in testes from 7 PCW onwards. However, several genes, such as *CYP17A1, CYP11A1*, hydroxy-delta-5-steroid dehydrogenase, 3 beta- and steroid delta-isomerase 2 (*HSD3B2*) and hydroxysteroid 17-beta dehydrogenase 3 (*HSD17B3*), actually exhibited sexual dimorphism as early as 6 PCW, suggestive of an earlier induction of the molecular networks underlying Leydig cell differentiation. A more likely explanation could be that even if they are expressed only in Leydig cells later in development, (pre-)Sertoli cells may also express such factors in early stages. This would be in line with the described co-operation between these two cell types for the synthesis of androgens in the mouse fetal testis (O'Shaughnessy *et al.*, 2000; Shima *et al.*, 2013) at 6 PCW. Among male-biased early-SDTs we also identified expression patterns similar to that of *SRY,* such as for the Wnt ligand secretion mediator (*WLS*) and for the C-C motif chemokine receptor 1 (*CCR1*). *WLS*, which we found to be preferentially expressed in fetal Sertoli cells, is an important mediator of Wnt secretion (Bänziger *et al.*, 2006; Das *et al.*, 2012), suggesting a potential role in promoting sex determination. We found *CCR1* to be preferentially expressed in germ cells. This was rather surprising since a sexually-dimorphic expression pattern at such an early developmental stage (i.e. as early as 6PCW) is expected to result from primary changes

584 in expression in somatic cells as they commit to their male or female fates. CCR1 encodes a chemokine
585 receptor thought to be implicated in stem cell niche establishment and maintenance and it has already
586 been shown to be expressed in postnatal gonocytes in the mouse (Simon *et al.*, 2010). Although we
587 demonstrated the high quality of the sorted cell populations used in the current study, it cannot be
588 totally excluded that the germline expression of *CCR1* may indeed correspond to a contamination by
589 KIT-expressing somatic cells such as macrophages. Many other candidate genes display a *SOX9*-like
590 expression pattern suggesting that some of them could also be important for Sertoli cell differentiation.
591 Among these candidate genes, several are already known to be important for gonad development or
592 fertility in humans and/or mice, such as such as FATE1, MAGEB1 or SOX10. Interestingly, while we
593 found the expression pattern of SOX10 to be conserved between human and mouse (i.e. with strong
594 preferential expression in young fetal testes), that of SOX8 was not. Instead, we found SOX8 to be
595 expressed in a similar manner in human fetal testes and ovaries, with peak expression between 6 and
596 7 PWC followed by subsequent downregulation. While this expression profile is clearly not
597 incompatible with a role during early testis differentiation as in the mouse (Schepers *et al.*, 2003), it
598 also suggests a potential broader involvement in development of both XX and XY gonads in humans.
599 The role of other candidates, such as the Erb-b2 receptor tyrosine kinase 3 (*ERBB3*) and the EPH
600 receptor B1 (*EPHB1*), remains unknown during early gonad development. The expression of *ERBB3*
601 has been reported in mouse PGCs in the genital ridge suggesting that the ErbB signalling might
602 contribute to control of growth and survival of PGCs (Toyoda-Ohno *et al.*, 1999). The expression of
603 *EPHB1* has never been reported in the fetal testis but is involved in angiogenesis and neural
604 development (Pasquale, 2005).

605 Due to the limited number of known markers for distinct fetal ovarian somatic cells, the association of
606 female-biased expression patterns (P8-P14) with specific cell populations remains challenging at the
607 whole gonad level. We found that several PGC markers, such as *KIT*, *POU5F1*, *NANOG* or *LIN28A*,

608 are over-expressed in the ovary, compared with the testis, as early as 6 PCW. This is in line with the
609 fact that PGCs proliferate at a higher rate than somatic cells in the human fetal ovary (Bendsen *et al.*,
610 2003; Lutterodt *et al.*, 2009; Mamsen *et al.*, 2010). Experimental investigations allowed us to identify
611 candidate genes associated with the ovarian somatic cell lineages, such as SRY-box 4 (*SOX4*), SET
612 nuclear proto-oncogene (*SET*), contactin 1 (*CNTN1*), neurexin 3 (*NRXN3*) and neuropeptide Y (*NPY*).
613 This set of genes holds great promise as potential key factors for female sex determination and ovary
614 differentiation. *SOX4* encodes a transcription factor with a high mobility group box domain and its
615 expression has already been described in supporting cells of the mouse gonads, although without
616 evident sexual dimorphism (Zhao *et al.*, 2017). *SET*, for which we demonstrate a highly sexually
617 dimorphic expression as early as 6 PCW, is implicated in transcriptional regulation through
618 epigenomic modifications and has been associated with polycystic ovary syndrome (Jiang *et al.*, 2017).
619 Other candidate genes expressed in somatic cells appear to be implicated in neurogenesis, such as
620 *NRXN3*, *NPY* and *CNTN1* (Sutton *et al.*, 1988; Markiewicz *et al.*, 2003; Bizzoca *et al.*, 2012; Harkin
621 *et al.*, 2016). *NRXN3* is expressed at a very weak level in the human fetal brain between 8 and 12 PCW
622 (Harkin *et al.*, 2016) , i.e. 2 weeks after a high transcriptional induction in the fetal ovary at 6 PCW,
623 which may indicate an independent role of the gene in both processes. NPY is already known to control
624 female reproductive processes at the hypothalamus level, and to have a direct action on ovarian cell
625 proliferation and apoptosis in prepubertal gilts (Sirotkin *et al.*, 2015). In contrast, *CNTN1* encodes a
626 neuronal cell adhesion molecule that has never been described in reproductive-related processes, but
627 seems to be a key factor in the development of many cancers (Chen *et al.*, 2018). The role of these
628 three candidates in female developing gonads remains unknown. All of the above mentioned male-
629 biased (*WLS*, *CCR1*, *ERBB3*, *EPHB1*, *CITED1* and *asCITED1*) and female-biased (*SOX4*, *SET*,
630 *NRXN3* and *NPY*) candidate genes would require further functional experiments to untangle their role
631 during gonad development.

One of the most original contributions of our study is to unravel the non-coding counterpart of the fetal gonadal transcriptome. To the best of our knowledge, this is the first study to address this issue in humans. As mentioned before, we assembled 1,209 lncRNAs and 318 NUTs expressed in developing fetal gonads. The statistical comparison of their genomic features and a protein-encoding analysis strongly suggest that the vast majority of NUTs corresponds to newly identified lncRNAs. However, based on the PIT approach and the protein-encoding analyses, a small fraction (6.2%) of the identified noncoding transcripts are good candidates for novel protein-coding genes as they were confirmed at the protein level. Our RNA-seq analysis also contributed to the identification of 680 antisense lncRNAs, including one located on the opposite strand of the Cbp/p300 interacting transactivator with Glu/Asp rich carboxy-terminal domain 1 (*CITED1*). Both sense and antisense (*asCITED1*, *TCONS_00249587*) transcripts showed a preferential, highly correlated expression in fetal Sertoli cells as early as 6 PCW. In the mouse, *Cited1* has been reported to be a potential target of *Sry* (Li *et al.*, 2014) and is specifically expressed in the adult testis (Fagerberg *et al.*, 2014). Our results suggest that *asCITED1* might contribute to the regulation of *CITED1*, and could therefore be implicated in early testis development in humans. We also report an accumulation of lncRNAs in expression patterns associated with female meiosis (P13-P14). This result is line with similar observations that have been made in adult germ cells from meiosis onwards (Cabili *et al.*, 2011; Laiho *et al.*, 2013; Chalmel *et al.*, 2014; Rolland *et al.*, 2019). This phenomenon thus seems to be conserved in both male and female germ cells, which suggests that lncRNAs might also play critical roles in human fetal oocytes. Furthermore, we observed that the vast majority of noncoding early-SDTs (16/20 NUTs, and 28/40 lncRNAs) were preferentially expressed in fetal ovaries, which may reflect a specific non-coding transcriptional program at play during early ovary development. Further investigation allowed us to identify that early, female-biased NUTs were preferentially expressed in germ cells (*TCONS_00042656*, *TCONS_00055038*, *TCONS_00113718*) although some were also expressed in

somatic cells (*TCONS_00153406* and *TCONS_00224470*). Additional functional analysis will be essential to elucidate the role of these germline and somatic candidates in the physiology of the fetal developing gonads and in the aetiology of DSDs. DSDs indeed comprise heterogeneous conditions affecting the genital system, with a wide range of phenotypes. The management of these disorders is globally improved by genetic diagnosis, as it leads to a more accurate prognosis and prediction of the long-term outcome. Recently, recommendations from the European Cooperation in Science and Technology state that genetic diagnosis should preferentially use whole exome sequencing of a panel of candidate genes, while whole genome sequencing should be restricted to suspected oligo- or poly-genic DSDs (Audí *et al.*, 2018). Nevertheless, the majority of genetic testing remains inconclusive as most causative genes involved in DSDs have not yet been identified (Alhomaidah *et al.*, 2017). Although many challenges remain to understand the implications of lncRNAs during gonad development in humans, their functional roles in almost all investigated biological systems are now supported by several studies (Cheng *et al.*, 2016; Tao *et al.*, 2016), including during gonad development (Rastetter *et al.*, 2015; Taylor *et al.*, 2015; Winge *et al.*, 2017) and for gonadal functions (Ohhata *et al.*, 2011; Bao *et al.*, 2013; Taylor *et al.*, 2015; Watanabe *et al.*, 2015; Wen *et al.*, 2016; Hosono *et al.*, 2017; Wichman *et al.*, 2017; Jégu *et al.*, 2019). Genome-wide association studies of patients with DSD would therefore greatly benefit from screening for new causal genetic variants in lncRNAs expressed early in sex determination. In this context our resource will assist geneticists to refine and complete the required panel of disease candidate genes by including non-coding genes involved in testicular and ovarian dysgenesis syndromes with a fetal origin, including cryptorchidism and testicular cancers.

Single-cell technologies now open new avenues for the genomic characterization of biological systems, including the study of cellular heterogeneity. When compared to bulk approaches, single-cell transcriptomics allows transcriptional signatures to be robustly assigned to specific cell types. In this

fast-evolving field, however, distinct available technologies have specific advantages and limitations, and may be favoured depending on the scientific question (Baran-Gale *et al.*, 2018). For instance, high-throughput systems that enable the analysis of several thousands of cells, including the mature and popular droplet-based high-throughput system from 10x Genomics, are needed in order to study discrete cell populations and/or to accurately reconstruct cell differentiation processes. On the other hand these systems suffer from a relatively low sensitivity and specificity: they only capture a partial fraction of the transcriptome of each individual cell (~2-4,000 genes per cell). Furthermore, by focusing on either the 3' or the 5' extremity of RNA molecules, they do not allow the reconstruction of transcript isoforms or the discovery of new genes. In the near future, increased sensitivity of droplet-based methods, combined with long-read sequencing technologies, will provide accurate transcriptome information at the isoform level and at a single-cell resolution (Byrne *et al.*, 2019), hopefully at an affordable price. In the meantime, bulk RNA-seq and current single-cell technologies remain highly complementary. The current study will support and complement future single-cell experiments aimed at reconstructing cell lineage progression in fetal gonads.

Overall, our study comprehensively describes the dynamic transcriptional landscape of the fetal gonads at seven key developmental stages in humans. This work discovered extensive sexually and non-sexually dimorphic expression changes, not only of protein-coding genes but also of lncRNAs and novel genes that are triggered early during gonad differentiation. This rich resource significantly extends existing state of the art knowledge and constitutes an invaluable reference atlas for the field of reproductive sciences and sex determination in particular.

Acknowledgments

We thank all members of the SEQanswers forums for helpful advice; Steven Salzberg and Cole Trapnell for continuous support with the "Tuxedo" suite; and the UCSC Genome team members. Sequencing was performed by the GenomEast platform, a member of the 'France Génomique' consortium (ANR-10-INBS-0009). We thank Ms Linda Robertson, Ms Margaret Fraser, Ms Samantha Flannigan (University of Aberdeen) and the staff at Grampian NHS Pregnancy Counselling Service, and all the staff of the Department of Obstetrics and Gynecology of the Rennes Sud Hospital for their expert assistance and help, and the participating women, without whom this study would not have been possible. The authors are grateful for Ms Gersende Lacombe and Mr Laurent Deleurme from the Biosit CytomeTri cytometry core facility of Rennes 1 University.

Authors' roles

FC, ADR, SMG and BJ designed the study. FC, ADR and EL wrote the manuscript. FC and ADR supervised the research. EL and FC prepared, analysed, and interpreted data. ADR, SMG, IC, MBM, PF, PAF, SLP, and BJ prepared the samples and interpreted sequencing data. BE, ADR and SMG validated expression data. SMG, PF, PAF and BJ contributed to the manuscript. All authors approved the final version of the manuscript.

Funding

This work was supported by the French National Institute of Health and Medical Research (Inserm), the University of Rennes 1, the French School of Public Health (EHESP), the Swiss National Science Foundation [SNF n° CRS115_171007 to B.J.], the French National Research Agency [ANR n° 16-CE14-0017-02 and n°18-CE14-0038-02 to F.C], the Medical Research Council [MR/L010011/1 to PAF] and the European Community's Seventh Framework Programme (FP7/2007-2013) [under grant

725 agreement no 212885 to PAF] and from the European Union's Horizon 2020 Research and Innovation
726 Programme [under grant agreement no 825100 to PAF and SMG]. The authors have no competing
727 financial interests.

728

729 **Conflict of interest**

730 There are no competing interests related to this study.

731

References

Adusumilli R, Mallick P. Data Conversion with ProteoWizard msConvert. *Methods Mol Biol* [Internet] 2017;**1550**:, p. 339–368.

Akane A, Seki S, Shiono H, Nakamura H, Hasegawa M, Kagawa M, Matsubara K, Nakahori Y, Nagafuchi S, Nakagome Y. Sex determination of forensic samples by dual PCR amplification of an X-Y homologous gene. *Forensic Sci Int* [Internet] 1992;**52**:143–148.

Alhomaidah D, McGowan R, Ahmed SF. The current state of diagnostic genetics for conditions affecting sex development. *Clin Genet* [Internet] 2017;**91**:157–162. Blackwell Publishing Ltd.

Audí L, Ahmed SF, Krone N, Cools M, McElreavey K, Holterhus PM, Greenfield A, Bashamboo A, Hiort O, Wudy SA, *et al.* GENETICS IN ENDOCRINOLOGY: Approaches to molecular genetic diagnosis in the management of differences/disorders of sex development (DSD): position paper of EU COST Action BM 1303 'DSDnet.' *Eur J Endocrinol* [Internet] 2018;**179**:R197–R206.

Bagheri-Fam S, Bird AD, Zhao L, Ryan JM, Yong M, Wilhelm D, Koopman P, Eswarakumar VP, Harley VR. Testis Determination Requires a Specific FGFR2 Isoform to Repress FOXL2. *Endocrinology* [Internet] 2017;**158**:3832–3843. Oxford University Press.

Bänziger C, Soldini D, Schütt C, Zipperlen P, Hausmann G, Basler K. Wntless, a Conserved Membrane Protein Dedicated to the Secretion of Wnt Proteins from Signaling Cells. *Cell* [Internet] 2006;**125**:509–522.

Bao J, Wu J, Schuster AS, Hennig GW, Yan W. Expression profiling reveals developmentally regulated lncRNA repertoire in the mouse male germline. *Biol Reprod* [Internet] 2013;**89**:107. Society for the Study of Reproduction.

Baran-Gale J, Chandra T, Kirschner K. Experimental design for single-cell RNA sequencing. *Brief Funct Genomics* [Internet] 2018;**17**:233–239. Oxford University Press.

Bendsen E, Byskov AG, Laursen SB, Larsen H-PE, Andersen CY, Westergaard LG. Number of germ

cells and somatic cells in human fetal testes during the first weeks after sex differentiation. *Hum Reprod* [Internet] 2003;**18**:13–18.

Beverdam A, Koopman P. Expression profiling of purified mouse gonadal somatic cells during the critical time window of sex determination reveals novel candidate genes for human sexual dysgenesis syndromes. *Hum Mol Genet* [Internet] 2006;**15**:417–431. Oxford University Press.

Bizzoca A, Corsi P, Polizzi A, Pinto MF, Xenaki D, Furley AJW, Gennarini G. F3/Contactin acts as a modulator of neurogenesis during cerebral cortex development. *Dev Biol* [Internet] 2012;**365**:133–151.

Bouffant R Le, Guerquin MJ, Duquenne C, Frydman N, Coffigny H, Rouiller-Fabre V, Frydman R, Habert R, Livera G. Meiosis initiation in the human ovary requires intrinsic retinoic acid synthesis. *Hum Reprod* [Internet] 2010;**25**:2579–2590.

Bouma GJ, Affourtit JJP, Bult CJ, Eicher EM. *Transcriptional profile of mouse pre-granulosa and Sertoli cells isolated from early-differentiated fetal gonads* [Internet]. *Gene Expr Patterns* [Internet] 2007;**7**:113–123.

Bouma GJ, Hudson QJ, Washburn LL, Eicher EM. New Candidate Genes Identified for Controlling Mouse Gonadal Sex Determination and the Early Stages of Granulosa and Sertoli Cell Differentiation1. *Biol Reprod* [Internet] 2010;**82**:380–389.

Brown GR, Hem V, Katz KS, Ovetsky M, Wallin C, Ermolaeva O, Tolstoy I, Tatusova T, Pruitt KD, Maglott DR, *et al.* Gene: a gene-centered information resource at NCBI. *Nucleic Acids Res* [Internet] 2015;**43**:D36–D42.

Byrne A, Cole C, Volden R, Vollmers C. Realizing the potential of full-length transcriptome sequencing. *Philos Trans R Soc Lond B Biol Sci* [Internet] 2019;**374**:20190097. Royal Society Publishing.

Cabili MN, Trapnell C, Goff L, Koziol M, Tazon-Vega B, Regev A, Rinn JL. Integrative annotation

of human large intergenic noncoding RNAs reveals global properties and specific subclasses. *Genes Dev* [Internet] 2011;**25**:1915–1927. Cold Spring Harbor Laboratory Press.

Chalmel F, Lardenois a., Evrard B, Rolland a. D, Sallou O, Dumargne M-C, Coiffec I, Collin O, Primig M, Jegou B. High-Resolution Profiling of Novel Transcribed Regions During Rat Spermatogenesis. *Biol Reprod* [Internet] 2014;**91**:5–5.

Chalmel F, Primig M. The Annotation, Mapping, Expression and Network (AMEN) suite of tools for molecular systems biology. *BMC Bioinformatics* [Internet] 2008;**9**:86. BioMed Central.

Chang H, Gao F, Guillou F, Taketo MM, Huff V, Behringer RR. Wt1 negatively regulates beta-catenin signaling during testis development. *Development* [Internet] 2008;**135**:1875–1885.

Chassot A-A, Ranc F, Gregoire EP, Roepers-Gajadien HL, Taketo MM, Camerino G, Rooij DG de, Schedl A, Chaboissier M-C. Activation of -catenin signaling by Rspo1 controls differentiation of the mammalian ovary. *Hum Mol Genet* [Internet] 2008;**17**:1264–1277.

Chen N, He S, Geng J, Song Z-J, Han P-H, Qin J, Zhao Z, Song Y-C, Wang H-X, Dang C-X. Overexpression of Contactin 1 promotes growth, migration and invasion in Hs578T breast cancer cells. *BMC Cell Biol* [Internet] 2018;**19**:5.

Cheng L, Ming H, Zhu M, Wen B. Long noncoding RNAs as Organizers of Nuclear Architecture. *Sci China Life Sci* [Internet] 2016;**59**:236–244.

Childs AJ, Cowan G, Kinnell HL, Anderson RA, Saunders PTK. Retinoic Acid Signalling and the Control of Meiotic Entry in the Human Fetal Gonad. In Clarke H, editor. *PLoS One* [Internet] 2011;**6**:e20249.

Chocu S, Evrard B, Lavigne R, Rolland AD, Aubry F, Jégou B, Chalmel F, Pineau C. Forty-Four Novel Protein-Coding Loci Discovered Using a Proteomics Informed by Transcriptomics (PIT) Approach in Rat Male Germ Cells1. *Biol Reprod* [Internet] 2014;**91**:123–123.

Darde TA, Lecluze E, Lardenois A, Stévant I, Alary N, Tüttelmann F, Collin O, Nef S, Jégou B,

804 Rolland AD, *et al.* The ReproGenomics Viewer: a multi-omics and cross-species resource
805 compatible with single-cell studies for the reproductive science community. *Bioinformatics*
806 [Internet] 2019;Available from: http://www.ncbi.nlm.nih.gov/pubmed/30668675.
807 Darde TA, Sallou O, Becker E, Evrard B, Monjeaud C, Bras Y Le, Jégou B, Collin O, Rolland AD,
808 Chalmel F. The ReproGenomics Viewer: an integrative cross-species toolbox for the reproductive
809 science community. *Nucleic Acids Res* [Internet] 2015;**43**:W109-16. Oxford University Press.
810 Das S, Yu S, Sakamori R, Stypulkowski E, Gao N. Wntless in Wnt secretion: molecular, cellular and
811 genetic aspects. *Front Biol (Beijing)* [Internet] 2012;**7**:587–593. NIH Public Access.
812 Dehlin HM, Levick SP. Substance P in heart failure: The good and the bad. *Int J Cardiol* [Internet]
813 2014;**170**:270–277.
814 Eggers S, Sadedin S, Bergen JA van den, Robevska G, Ohnesorg T, Hewitt J, Lambeth L, Bouty A,
815 Knarston IM, Tan TY, *et al.* Disorders of sex development: insights from targeted gene
816 sequencing of a large international patient cohort. *Genome Biol* [Internet] 2016;**17**:243.
817 Evans VC, Barker G, Heesom KJ, Fan J, Bessant C, Matthews DA. De novo derivation of proteomes
818 from transcriptomes for transcript and protein identification. *Nat Methods* [Internet]
819 2012;**9**:1207–1211.
820 Evtouchenko L, Studer L, Spencer C, Dreher E, Seiler RW. A mathematical model for the estimation
821 of human embryonic and fetal age. *Cell Transplant* [Internet] 1996;**5**:453–464.
822 Fagerberg L, Hallström BM, Oksvold P, Kampf C, Djureinovic D, Odeberg J, Habuka M,
823 Tahmasebpoor S, Danielsson A, Edlund K, *et al.* Analysis of the human tissue-specific expression
824 by genome-wide integration of transcriptomics and antibody-based proteomics. *Mol Cell*
825 *Proteomics* [Internet] 2014;**13**:397–406.
826 Finn RD, Clements J, Eddy SR. HMMER web server: interactive sequence similarity searching.
827 *Nucleic Acids Res* [Internet] 2011;**39**:W29-37.

828 Fowler PA, Cassie S, Rhind SM, Brewer MJ, Collinson JM, Lea RG, Baker PJ, Bhattacharya S,
829 O'Shaughnessy PJ. Maternal Smoking during Pregnancy Specifically Reduces Human Fetal
830 Desert Hedgehog Gene Expression during Testis Development. *J Clin Endocrinol Metab*
831 [Internet] 2008;**93**:619–626.
832 Fowler PA, Flannigan S, Mathers A, Gillanders K, Lea RG, Wood MJ, Maheshwari A, Bhattacharya
833 S, Collie-Duguid ESR, Baker PJPJ, *et al.* Gene expression analysis of human fetal ovarian
834 primordial follicle formation. *J Clin Endocrinol Metab* [Internet] 2009;**94**:1427–1435.
835 Friel A, Houghton JA, Glennon M, Lavery R, Smith T, Nolan A, Maher M. A preliminary report on
836 the implication of RT-PCR detection of DAZ, RBMY1, USP9Y and Protamine-2 mRNA in
837 testicular biopsy samples from azoospermic men. *Int J Androl* [Internet] 2002;**25**:59–64.
838 Gkountela S, Zhang KXX, Shafiq TAA, Liao W-WW, Hargan-Calvopi??a J, Chen P-YY, Clark ATT,
839 Hargan-Calvopiña J, Chen P-YY, Clark ATT, *et al.* DNA demethylation dynamics in the human
840 prenatal germline. *Cell* [Internet] 2015;**161**:1425–1436.
841 Greenfield A. Understanding sex determination in the mouse: genetics, epigenetics and the story of
842 mutual antagonisms. *J Genet* [Internet] 2015;**94**:585–590.
843 Guo F, Yan L, Guo H, Li L, Hu B, Zhao Y, Yong J, Hu Y, Wang X, Wei Y, *et al.* The transcriptome
844 and DNA methylome landscapes of human primordial germ cells. *Cell* [Internet] 2015;**161**:1437–
845 1452. Elsevier Inc.
846 Guo H, Hu B, Yan L, Yong J, Wu Y, Gao Y, Guo F, Hou Y, Fan X, Dong J, *et al.* DNA methylation
847 and chromatin accessibility profiling of mouse and human fetal germ cells. *Cell Res* [Internet]
848 2017;**27**:165–183. Nature Publishing Group.
849 Han H, Shim H, Shin D, Shim JE, Ko Y, Shin J, Kim HH, Cho A, Kim E, Lee T, *et al.* TRRUST: a
850 reference database of human transcriptional regulatory interactions. *Sci Rep* [Internet]
851 2015;**5**:11432. Nature Publishing Group.

852 Hanley N., Hagan D., Clement-Jones M, Ball S. S, Strachan T, Salas-Cortés L, McElreavey K, Lindsay
853 S, Robson S, Bullen P, *et al.* SRY, SOX9, and DAX1 expression patterns during human sex
854 determination and gonadal development. *Mech Dev* [Internet] 2000;**91**:403–407.
855 Hanley NA, Ball SG, Clement-Jones M, Hagan DM, Strachan T, Lindsay S, Robson S, Ostrer H,
856 Parker KL, Wilson DI. Expression of steroidogenic factor 1 and Wilms' tumour 1 during early
857 human gonadal development and sex determination. *Mech Dev* 1999;**87**:175–180.
858 Haque A, Engel J, Teichmann SA, Lönnberg T. A practical guide to single-cell RNA-sequencing for
859 biomedical research and clinical applications. *Genome Med* [Internet] 2017;**9**:75.
860 Harkin LF, Lindsay SJ, Xu Y, Alzu'bi A, Ferrara A, Gullon EA, James OG, Clowry GJ. Neurexins 1–
861 3 Each Have a Distinct Pattern of Expression in the Early Developing Human Cerebral Cortex.
862 *Cereb Cortex* [Internet] 2016;**278**:4497–4505. Oxford University Press.
863 Hastie ND. Wilms' tumour 1 (WT1) in development, homeostasis and disease. *Development* [Internet]
864 2017;**144**:2862–2872.
865 Hogeveen KN, Sassone-Corsi P. Regulation of gene expression in post-meiotic male germ cells:
866 CREM-signalling pathways and male fertility. *Hum Fertil (Camb)* [Internet] 2006;**9**:73–79.
867 Hosono Y, Niknafs YS, Prensner JR, Iyer MK, Dhanasekaran SM, Mehra R, Pitchiaya S, Tien J,
868 Escara-Wilke J, Poliakov A, *et al.* Oncogenic Role of THOR, a Conserved Cancer/Testis Long
869 Non-coding RNA. *Cell* [Internet] 2017;**171**:1559-1572.e20.
870 Houmard B, Small C, Yang L, Naluai-Cecchini T, Cheng E, Hassold T, Griswold M. Global Gene
871 Expression in the Human Fetal Testis and Ovary. *Biol Reprod* [Internet]
872 2009;**443**:biolreprod.108.075747.
873 Inoue M, Shima Y, Miyabayashi K, Tokunaga K, Sato T, Baba T, Ohkawa Y, Akiyama H, Suyama
874 M, Morohashi K. Isolation and Characterization of Fetal Leydig Progenitor Cells of Male Mice.
875 *Endocrinology* [Internet] 2016;**157**:1222–1233.

876 Jameson SA, Lin Y-T, Capel B. Testis development requires the repression of Wnt4 by Fgf signaling.
877 *Dev Biol* [Internet] 2012a;**370**:24–32.
878 Jameson SA, Natarajan A, Cool J, DeFalco T, Maatouk DM, Mork L, Munger SC, Capel B. Temporal
879 Transcriptional Profiling of Somatic and Germ Cells Reveals Biased Lineage Priming of Sexual
880 Fate in the Fetal Mouse Gonad. In Barsh GS, editor. *PLoS Genet* [Internet] 2012b;**8**:e1002575.
881 Public Library of Science.
882 Jégou B, Sankararaman S, Rolland AD, Reich D, Chalmel F. Meiotic Genes Are Enriched in Regions
883 of Reduced Archaic Ancestry. *Mol Biol Evol* [Internet] 2017;**34**:1974–1980.
884 Jégu T, Blum R, Cochrane JC, Yang L, Wang C-Y, Gilles M-E, Colognori D, Szanto A, Marr SK,
885 Kingston RE, *et al.* Xist RNA antagonizes the SWI/SNF chromatin remodeler BRG1 on the
886 inactive X chromosome. *Nat Struct Mol Biol* [Internet] 2019;**26**:96.
887 Jiang S-W, Xu S, Chen H, Liu X, Tang Z, Cui Y, Liu J. Pathologic significance of SET/I2PP2A-
888 mediated PP2A and non-PP2A pathways in polycystic ovary syndrome (PCOS). *Clin Chim Acta*
889 [Internet] 2017;**464**:155–159.
890 Jørgensen A, Macdonald J, Nielsen JE, Kilcoyne KR, Perlman S, Lundvall L, Langhoff Thuesen L,
891 Juul Hare K, Frederiksen H, Andersson AM, *et al.* Nodal Signaling Regulates Germ Cell
892 Development and Establishment of Seminiferous Cords in the Human Fetal Testis. *Cell Rep*
893 2018;**25**:1924-1937.e4. Elsevier B.V.
894 Kashimada K, Pelosi E, Chen H, Schlessinger D, Wilhelm D, Koopman P. FOXL2 and BMP2 act
895 cooperatively to regulate follistatin gene expression during ovarian development. *Endocrinology*
896 [Internet] 2011;**152**:272–280.
897 Kim J-H, Shin HS, Lee SH, Lee I, Lee YSYC, Park JC, Kim YJ, Chung JB, Lee YSYC. Contrasting
898 activity of Hedgehog and Wnt pathways according to gastric cancer cell differentiation: relevance
899 of crosstalk mechanisms. *Cancer Sci* [Internet] 2010;**101**:328–335.

900 Kim M-S, Pinto SM, Getnet D, Nirujogi RS, Manda SS, Chaerkady R, Madugundu AK, Kelkar DS,
901 Isserlin R, Jain S, *et al.* A draft map of the human proteome. *Nature* [Internet] 2014;**509**:575–
902 581.
903 Kim Y, Capel B. Balancing the bipotential gonad between alternative organ fates: A new perspective
904 on an old problem. *Dev Dyn* [Internet] 2006;**235**:2292–2300.
905 Kong L, Zhang Y, Ye Z-Q, Liu X-Q, Zhao S-Q, Wei L, Gao G. CPC: assess the protein-coding
906 potential of transcripts using sequence features and support vector machine. *Nucleic Acids Res*
907 [Internet] 2007;**35**:W345-9.
908 Koopman P, Gubbay J, Vivian N, Goodfellow P, Lovell-Badge R. Male development of
909 chromosomally female mice transgenic for Sry. *Nature* [Internet] 1991;**351**:117–121.
910 Kuhn RM, Haussler D, Kent WJ. The UCSC genome browser and associated tools. *Brief Bioinform*
911 [Internet] 2013;**14**:144–161.
912 Laiho A, Kotaja N, Gyenesei A, Sironen A. Transcriptome profiling of the murine testis during the
913 first wave of spermatogenesis. *PLoS One* [Internet] 2013;**8**:e61558. Public Library of Science.
914 Lê S, Josse J, Husson F. FactoMineR: An R Package for Multivariate Analysis. *J Stat Softw* [Internet]
915 2008;**25**:1–18.
916 Li H, Handsaker B, Wysoker A, Fennell T, Ruan J, Homer N, Marth G, Abecasis G, Durbin R, 1000
917 Genome Project Data Processing Subgroup. The Sequence Alignment/Map format and
918 SAMtools. *Bioinformatics* [Internet] 2009;**25**:2078–2079.
919 Li L, Dong J, Yan L, Yong J, Liu X, Hu Y, Fan X, Wu X, Guo H, Wang X, *et al.* Single-Cell RNA-
920 Seq Analysis Maps Development of Human Germline Cells and Gonadal Niche Interactions. *Cell*
921 *Stem Cell* [Internet] 2017;**20**:891–892.
922 Li Y, Zheng M, Lau Y-FC. *The Sex-Determining Factors SRY and SOX9 Regulate Similar Target*
923 *Genes and Promote Testis Cord Formation during Testicular Differentiation* [Internet]. *Cell Rep*

924 [Internet] 2014;**8**:723–733.
925 Liu C-F, Bingham N, Parker K, Yao HH-C. Sex-specific roles of β-catenin in mouse gonadal
926 development. *Hum Mol Genet* [Internet] 2009;**18**:405–417.
927 Lutterodt MC, Sørensen KP, Larsen KB, Skouby SO, Andersen CY, Byskov AG. The number of
928 oogonia and somatic cells in the human female embryo and fetus in relation to whether or not
929 exposed to maternal cigarette smoking. *Hum Reprod* [Internet] 2009;**24**:2558–2566.
930 Maatouk DM, DiNapoli L, Alvers A, Parker KL, Taketo MM, Capel B. Stabilization of β-catenin in
931 XY gonads causes male-to-female sex-reversal. *Hum Mol Genet* [Internet] 2008;**17**:2949–2955.
932 Mamsen LS, Ernst EHE, Borup R, Larsen A, Olesen RH, Ernst EHE, Anderson RA, Kristensen SG,
933 Andersen CY. Temporal expression pattern of genes during the period of sex differentiation in
934 human embryonic gonads. *Sci Rep* [Internet] 2017;**7**:15961. Nature Publishing Group.
935 Mamsen LS, Lutterodt MC, Andersen EW, Skouby SO, Sørensen KP, Andersen CY, Byskov AG.
936 Cigarette smoking during early pregnancy reduces the number of embryonic germ and somatic
937 cells. *Hum Reprod* [Internet] 2010;**25**:2755–2761.
938 Mantione KJ, Kream RM, Kuzelova H, Ptacek R, Raboch J, Samuel JM, Stefano GB. Comparing
939 bioinformatic gene expression profiling methods: microarray and RNA-Seq. *Med Sci Monit Basic*
940 *Res* [Internet] 2014;**20**:138–142. International Scientific Literature, Inc.
941 Markiewicz W, Jaroszewski JJ, Bossowska A, Majewski M. NPY: its occurrence and relevance in the
942 female reproductive system. *Folia Histochem Cytobiol* [Internet] 2003;**41**:183–192.
943 McClelland KS, Bell K, Larney C, Harley VR, Sinclair AH, Oshlack A, Koopman P, Bowles J.
944 Purification and Transcriptomic Analysis of Mouse Fetal Leydig Cells Reveals Candidate Genes
945 for Specification of Gonadal Steroidogenic Cells1. *Biol Reprod* [Internet] 2015;**92**:1–12. Oxford
946 University Press.
947 Munger SCS, Natarajan A, Looger LL, Ohler U, Capel B, Munger SCS, Aylor D, Syed H, Magwene

948 P, Threadgill D, *et al.* Fine Time Course Expression Analysis Identifies Cascades of Activation
949 and Repression and Maps a Putative Regulator of Mammalian Sex Determination. In Beier DR,
950 editor. *PLoS Genet* [Internet] 2013;**9**:e1003630. Public Library of Science.
951 Nef S, Schaad O, Stallings NR, Cederroth CR, Pitetti J-L, Schaer G, Malki S, Dubois-Dauphin M,
952 Boizet-Bonhoure B, Descombes P, *et al.* Gene expression during sex determination reveals a
953 robust female genetic program at the onset of ovarian development. *Dev Biol* [Internet]
954 2005;**287**:361–377.
955 O'Shaughnessy PJ, Antignac JP, Bizec B Le, Morvan ML, Svechnikov K, Söder O, Savchuk I,
956 Monteiro A, Soffientini U, Johnstonid ZC, *et al.* Alternative (Backdoor) androgen production and
957 masculinization in the human fetus. *PLoS Biol* 2019;**17**:. Public Library of Science.
958 O'Shaughnessy PJ, Baker PJ, Heikkilä M, Vainio S, McMahon AP. Localization of 17β-
959 Hydroxysteroid Dehydrogenase/17-Ketosteroid Reductase Isoform Expression in the Developing
960 Mouse Testis—Androstenedione Is the Major Androgen Secreted by Fetal/Neonatal Leydig Cells
961 [1]. *Endocrinology* [Internet] 2000;**141**:2631–2637.
962 O'Shaughnessy PJ, Baker PJJ, Monteiro A, Cassie S, Bhattacharya S, Fowler PA, O'Shaughnessy PJ,
963 Baker PJJ, Monteiro A, Cassie S, *et al.* Developmental changes in human fetal testicular cell
964 numbers and messenger ribonucleic acid levels during the second trimester. *J Clin Endocrinol*
965 *Metab* [Internet] 2007;**92**:4792–4801. Endocrine Society.
966 Ohhata T, Senner CE, Hemberger M, Wutz A. Lineage-specific function of the noncoding Tsix RNA
967 for Xist repression and Xi reactivation in mice. *Genes Dev* [Internet] 2011;**25**:1702–1715. Cold
968 Spring Harbor Laboratory Press.
969 Ostrer H, Huang HY, Masch RJ, Shapiro E. A cellular study of human testis development. *Sex Dev*
970 2007;**1**:286–292.
971 Ottolenghi C, Pelosi E, Tran J, Colombino M, Douglass E, Nedorezov T, Cao A, Forabosco A,

Schlessinger D. Loss of Wnt4 and Foxl2 leads to female-to-male sex reversal extending to germ cells. *Hum Mol Genet* [Internet] 2007;**16**:2795–2804.

Pasquale EB. Developmental cell biology: Eph receptor signalling casts a wide net on cell behaviour. *Nat Rev Mol Cell Biol* [Internet] 2005;**6**:462–475.

Pauli A, Valen E, Lin MF, Garber M, Vastenhouw NL, Levin JZ, Fan L, Sandelin A, Rinn JL, Regev A, *et al.* Systematic identification of long noncoding RNAs expressed during zebrafish embryogenesis. *Genome Res* [Internet] 2012;**22**:577–591.

Planells B, Gómez-Redondo I, Pericuesta E, Lonergan P, Gutiérrez-Adán A. Differential isoform expression and alternative splicing in sex determination in mice. *BMC Genomics* [Internet] 2019;**20**:.

Pollier J, Rombauts S, Goossens A. Analysis of RNA-Seq data with TopHat and Cufflinks for genome-wide expression analysis of jasmonate-treated plants and plant cultures. *Methods Mol Biol* [Internet] 2013;**1011**:305–315.

Prensner JR, Iyer MK, Balbin OA, Dhanasekaran SM, Cao Q, Brenner JC, Laxman B, Asangani IA, Grasso CS, Kominsky HD, *et al.* Transcriptome sequencing across a prostate cancer cohort identifies PCAT-1, an unannotated lincRNA implicated in disease progression. *Nat Biotechnol* [Internet] 2011;**29**:742–749.

Pruitt KD, Brown GR, Hiatt SM, Thibaud-Nissen F, Astashyn A, Ermolaeva O, Farrell CM, Hart J, Landrum MJ, McGarvey KM, *et al.* RefSeq: an update on mammalian reference sequences. *Nucleic Acids Res* [Internet] 2014;**42**:D756–D763.

Pundir S, Magrane M, Martin MJ, O'Donovan C, UniProt Consortium. Searching and Navigating UniProt Databases. *Curr Protoc Bioinforma* [Internet] 2015;**50**:1.27.1-10. John Wiley & Sons, Inc.: Hoboken, NJ, USA.

Qian J, Yehia G, Molina C, Fernandes A, Donnelly R, Anjaria D, Gascon P, Rameshwar P. Cloning

996 of human preprotachykinin-I promoter and the role of cyclic adenosine 5'-monophosphate
997 response elements in its expression by IL-1 and stem cell factor. *J Immunol (Baltimore, Md 1950)*
998 [Internet] 2001;**166**:2553–2561.
999 Rahmoun M, Lavery R, Laurent-Chaballier S, Bellora N, Philip GK, Rossitto M, Symon A, Pailhoux
000 E, Cammas F, Chung J, *et al.* In mammalian foetal testes, SOX9 regulates expression of its target
001 genes by binding to genomic regions with conserved signatures. *Nucleic Acids Res* [Internet]
002 2017;**45**:7191–7211.
003 Rastetter RH, Smith CA, Wilhelm D. The role of non-coding RNAs in male sex determination and
004 differentiation. *Reproduction* [Internet] 2015;**150**:R93-107. Society for Reproduction and
005 Fertility.
006 Rice P, Longden I, Bleasby A. EMBOSS: the European Molecular Biology Open Software Suite.
007 *Trends Genet* [Internet] 2000;**16**:276–277.
008 Rolland AD, Evrard B, Darde TA, Béguec C Le, Bras Y Le, Bensalah K, Lavoué S, Jost B, Primig M,
009 Dejucq-Rainsford N, *et al.* RNA profiling of human testicular cells identifies syntenic lncRNAs
010 associated with spermatogenesis. *Hum Reprod* [Internet] 2019;Available from:
011 http://www.ncbi.nlm.nih.gov/pubmed/31247106.
012 Rolland AD, Lehmann KP, Johnson KJ, Gaido KW, Koopman P. Uncovering gene regulatory
013 networks during mouse fetal germ cell development. *Biol Reprod* [Internet] 2011;**84**:790–800.
014 Society for the Study of Reproduction.
015 Santa Barbara P de, Méjean C, Moniot B, Malclès MH, Berta P, Boizet-Bonhoure B. Steroidogenic
016 factor-1 contributes to the cyclic-adenosine monophosphate down-regulation of human SRY gene
017 expression. *Biol Reprod* [Internet] 2001;**64**:775–783.
018 Schepers G, Wilson M, Wilhelm D, Koopman P. SOX8 Is Expressed during Testis Differentiation in
019 Mice and Synergizes with SF1 to Activate the *Amh* Promoter *in Vitro*. *J Biol Chem* [Internet]

2003;**278**:28101–28108.

Schmidt D. The murine winged-helix transcription factor Foxl2 is required for granulosa cell differentiation and ovary maintenance. *Development* [Internet] 2004;**131**:933–942.

Sekido R, Lovell-Badge R. Sex determination involves synergistic action of SRY and SF1 on a specific Sox9 enhancer. *Nature* [Internet] 2008;**453**:930–934. Nature Publishing Group.

Shima Y, Miyabayashi K, Haraguchi S, Arakawa T, Otake H, Baba T, Matsuzaki S, Shishido Y, Akiyama H, Tachibana T, *et al.* Contribution of Leydig and Sertoli Cells to Testosterone Production in Mouse Fetal Testes. *Mol Endocrinol* [Internet] 2013;**27**:63–73.

Simon L, Ekman GC, Garcia T, Carnes K, Zhang Z, Murphy T, Murphy KM, Hess RA, Cooke PS, Hofmann M. ETV5 Regulates Sertoli Cell Chemokines Involved in Mouse Stem/Progenitor Spermatogonia Maintenance. *Stem Cells* [Internet] 2010;**28**:1882–1892.

Sirotkin A V, Kardošová D, Alwasel SH, Harrath AH. Neuropeptide Y directly affects ovarian cell proliferation and apoptosis. *Reprod Biol* [Internet] 2015;**15**:257–260.

Small CL, Shima JE, Uzumcu M, Skinner MK, Griswold MD. Profiling Gene Expression During the Differentiation and Development of the Murine Embryonic Gonad. *Biol Reprod* [Internet] 2005;**72**:492–501. NIH Public Access.

Smyth GK. Linear Models and Empirical Bayes Methods for Assessing Differential Expression in Microarray Experiments. *Stat Appl Genet Mol Biol* [Internet] 2004;**3**:1–25.

Sorby-Adams AJ, Marcoionni AM, Dempsey ER, Woenig JA, Turner RJ. The Role of Neurogenic Inflammation in Blood-Brain Barrier Disruption and Development of Cerebral Oedema Following Acute Central Nervous System (CNS) Injury. *Int J Mol Sci* [Internet] 2017;**18**:.

Speir ML, Zweig AS, Rosenbloom KR, Raney BJ, Paten B, Nejad P, Lee BT, Learned K, Karolchik D, Hinrichs AS, *et al.* The UCSC Genome Browser database: 2016 update. *Nucleic Acids Res* [Internet] 2016;**44**:D717–D725.

044 Stévant I, Kühne F, Greenfield A, Chaboissier M-C, Dermitzakis ET, Nef S. Dissecting Cell Lineage
045 Specification and Sex Fate Determination in Gonadal Somatic Cells Using Single-Cell
046 Transcriptomics. *Cell Rep* [Internet] 2019;**26**:3272-3283.e3.
047 Stévant I, Neirijnck Y, Borel C, Escoffier J, Smith LB, Antonarakis SE, Dermitzakis ET, Nef S.
048 Deciphering Cell Lineage Specification during Male Sex Determination with Single-Cell RNA
049 Sequencing. *Cell Rep* [Internet] 2018;**22**:1589–1599.
050 Sun J, Bhatia M. Substance P at the neuro-immune crosstalk in the modulation of inflammation, asthma
051 and antimicrobial host defense. *Inflamm Allergy Drug Targets* [Internet] 2014;**13**:112–120.
052 Sutton SW, Toyama TT, Otto S, Plotsky PM. Evidence that neuropeptide Y (NPY) released into the
053 hypophysial-portal circulation participates in priming gonadotropes to the effects of gonadotropin
054 releasing hormone (GnRH). *Endocrinology* [Internet] 1988;**123**:1208–1210.
055 Svingen T, Jørgensen A, Rajpert-De Meyts E. Validation of endogenous normalizing genes for
056 expression analyses in adult human testis and germ cell neoplasms. *Mol Hum Reprod*
057 2014;**20**:709–718.
058 Tao S, Xiu-Lei Z, Xiao-Lin L, Sai-Nan M, Yu-Zhu G, Xiang-Ting W. Recent Progresses of Long
059 Noncoding RNA. *Biomed Sci* [Internet] 2016;**1**:34.
060 Taylor DH, Chu ET-J, Spektor R, Soloway PD. Long non-coding RNA regulation of reproduction and
061 development. *Mol Reprod Dev* [Internet] 2015;**82**:932–956. NIH Public Access.
062 Toyoda-Ohno H, Obinata M, Matsui Y. Members of the ErbB receptor tyrosine kinases are involved
063 in germ cell development in fetal mouse gonads. *Dev Biol* [Internet] 1999;**215**:399–406.
064 Trapnell C, Roberts A, Goff L, Petrea G, Kim D, Kelley DR, Pimentel H, Salzberg S, Rinn JL, Pachter
065 L. Differential gene and transcript expressiont analysis of RNA-seq experiments with TopHat and
066 Cufflinks. *Natures Protoc* 2012;**7**:562–578.
067 Uda M, Ottolenghi C, Crisponi L, Garcia JE, Deiana M, Kimber W, Forabosco A, Cao A, Schlessinger

068 D, Pilia G. Foxl2 disruption causes mouse ovarian failure by pervasive blockage of follicle
069 development. *Hum Mol Genet* [Internet] 2004;**13**:1171–1181.
070 Vainio S, Heikkilä M, Kispert A, Chin N, McMahon AP. Female development in mammals is regulated
071 by Wnt-4 signalling. *Nature* [Internet] 1999;**397**:405–409.
072 Valle I del, Buonocore F, Duncan AJ, Lin L, Barenco M, Parnaik R, Shah S, Hubank M, Gerrelli D,
073 Achermann JC. A genomic atlas of human adrenal and gonad development. *Wellcome Open Res*
074 [Internet] 2017;**2**:25.
075 Vaudel M, Barsnes H, Berven FS, Sickmann A, Martens L. SearchGUI: An open-source graphical user
076 interface for simultaneous OMSSA and X!Tandem searches. *Proteomics* 2011;**11**:996–999.
077 Vaudel M, Burkhart JM, Zahedi RP, Oveland E, Berven FS, Sickmann A, Martens L, Barsnes H.
078 PeptideShaker enables reanalysis of MS-derived proteomics data sets. *Nat Biotechnol* [Internet]
079 2015;**33**:22–24.
080 Vidal VPI, Chaboissier M-C, Rooij DG de, Schedl A. Sox9 induces testis development in XX
081 transgenic mice. *Nat Genet* [Internet] 2001;**28**:216–217.
082 Vizcaíno JA, Csordas A, del-Toro N, Dianes JA, Griss J, Lavidas I, Mayer G, Perez-Riverol Y,
083 Reisinger F, Ternent T, *et al.* 2016 update of the PRIDE database and its related tools. *Nucleic*
084 *Acids Res* [Internet] 2016;**44**:11033. Oxford University Press.
085 Wang L, Park HJ, Dasari S, Wang S, Kocher J-P, Li W. CPAT: Coding-Potential Assessment Tool
086 using an alignment-free logistic regression model. *Nucleic Acids Res* [Internet] 2013;**41**:e74.
087 Warr N, Siggers P, Bogani D, Brixey R, Pastorelli L, Yates L, Dean CH, Wells S, Satoh W, Shimono
088 A, *et al.* Sfrp1 and Sfrp2 are required for normal male sexual development in mice. *Dev Biol*
089 [Internet] 2009;**326**:273–284.
090 Watanabe T, Cheng E, Zhong M, Lin H. Retrotransposons and pseudogenes regulate mRNAs and
091 lncRNAs via the piRNA pathway in the germline. *Genome Res* [Internet] 2015;**25**:368–380. Cold

092 Spring Harbor Laboratory Press.
093 Wen K, Yang L, Xiong T, Di C, Ma D, Wu M, Xue Z, Zhang X, Long L, Zhang W, *et al.* Critical roles
094 of long noncoding RNAs in Drosophila spermatogenesis. *Genome Res* [Internet] 2016;**26**:1233–
095 1244.
096 Wichman L, Somasundaram S, Breindel C, Valerio DM, McCarrey JR, Hodges CA, Khalil AM.
097 Dynamic expression of long noncoding RNAs reveals their potential roles in spermatogenesis and
098 fertility. *Biol Reprod* [Internet] 2017;**97**:313–323. Oxford University Press.
099 Wilhelm D, Washburn LL, Truong V, Fellous M, Eicher EM, Koopman P. Antagonism of the testis-
100 and ovary-determining pathways during ovotestis development in mice. *Mech Dev* [Internet]
101 2009;**126**:324–336.
102 Wilhelm D, Yang JX, Thomas P. Mammalian sex determination and gonad development. In Thomas
103 P, editor. *Curr Top Dev Biol* [Internet] 2013;**106**:, p. 89–121. Academic Press.
104 Winge SB, Dalgaard MD, Jensen JM, Graem N, Schierup MH, Juul A, Rajpert-De Meyts E, Almstrup
105 K. Transcriptome profiling of fetal Klinefelter testis tissue reveals a possible involvement of long
106 non-coding RNAs in gonocyte maturation. *Hum Mol Genet* [Internet] 2017;**27**:430–439.
107 Wu R, Su Y, Wu H, Dai Y, Zhao M, Lu Q. Characters, functions and clinical perspectives of long non-
108 coding RNAs. *Mol Genet Genomics* [Internet] 2016;**291**:1013–1033.
109 Yates A, Akanni W, Amode MR, Barrell D, Billis K, Carvalho-Silva D, Cummins C, Clapham P,
110 Fitzgerald S, Gil L, *et al.* Ensembl 2016. *Nucleic Acids Res* [Internet] 2016;**44**:D710–D716.
111 Yusuf D, Butland SL, Swanson MI, Bolotin E, Ticoll A, Cheung WA, Zhang XYC, Dickman CTD,
112 Fulton DL, Lim JS, *et al.* The transcription factor encyclopedia. *Genome Biol* [Internet]
113 2012;**13**:R24. BioMed Central.
114 Zhao L, Arsenault M, Ng ET, Longmuss E, Chau TC-Y, Hartwig S, Koopman P. SOX4 regulates
115 gonad morphogenesis and promotes male germ cell differentiation in mice. *Dev Biol* [Internet]

2017;**423**:46–56.

Zhao L, Wang C, Lehman ML, He M, An J, Svingen T, Spiller CM, Ng ET, Nelson CC, Koopman P. Transcriptomic analysis of mRNA expression and alternative splicing during mouse sex determination. *Mol Cell Endocrinol* [Internet] 2018;Available from: http://www.sciencedirect.com/science/article/pii/S030372071830234X.

Zimmermann C, Stévant I, Borel C, Conne B, Pitetti J-L, Calvel P, Kaessmann H, Jégou B, Chalmel F, Nef S. Research Resource: The Dynamic Transcriptional Profile of Sertoli Cells During the Progression of Spermatogenesis. *Mol Endocrinol* [Internet] 2015;**29**:627–642.

125 **Figure legends**

126 **Figure 1** Sample collection and assessment of homogeneity.

127 (A) Human fetal gonads used in this study were collected at seven developmental stages, i.e. at 6, early
128 7, late 7, 9, 12, 13–14 and 17 postconceptional week (PCW). The number of replicates is indicated for
129 each stage and sex. An overview of the main differentiation processes within human fetal testes and
130 ovaries during the studied time window is also provided. PGC = primordial germ cell; LC = Leydig
131 cell. The panel (B) displays the correlation (R^2) of the first 10 dimensions of principal component
132 analysis (PCA) with the development stage and the genetic sex. The PCA was performed on expression
133 data from 35,194 refined transcripts across all 48 human fetal gonads. Red values represent significant
134 correlations (p-value $\leqslant$ 1%). (C) A scatter plot represents the position of each sample along the first
135 two dimensions. Smaller dots represent samples, and are linked to bigger dots that represent the
136 average expression of transcripts across replicates. The histogram represents the percentage of
137 information carried by each dimension of the PCA. Testis samples are colored in blue, while ovaries
138 are in red. Time point of each condition is provided in PCW. e7 = early 7 PCW; l7 = late 7 PCW. The
139 variability between the samples is mainly explained by their age of development (dimension 1) and by
140 their genetic sex (dimension 2). The two arrows highlight the divergence of gonads transcriptomes,
141 from a common origin (at 6 PCW) to their distinct fate. (D) A dendrogram shows the hierarchical
142 relationship between the 48 samples. The hierarchical clustering is based on the 35 first PCA
143 dimensions explaining 90% of the total variance of the data. Male samples are colored in blue, female
144 samples are in red. (E) Coding potential analysis of refined transcripts. The combined results of the
145 Protein-Encoding Potential (PEP) and the Proteomics Informed by Transcriptomic (PIT) strategies, i.e.
146 Low or High PEP transcripts with (PIT+) or without (PIT-) identified peptide(s) are represented for
147 each transcript biotype. (F) Two statistical filtrations were used to select differentially-expressed
148 transcripts. First, we performed an “intra-sex” comparison in which all developmental stages were

compared to each other during testis development on the one hand, and during ovarian development on the other hand (Fold-change ⩾2 in at least one comparison). Second, we performed an "inter-sex" comparison in which testes and ovaries were compared at each developmental stage (Fold-change ⩾ 2 in at least one comparison). Subsequently, a linear models for microarray data (LIMMA) statistical test was performed on both sets of transcripts to select those with significant expression variation across replicates [false discovery rate (FDR)-adjusted F-value of ⩽ 0.05]. A total of 13,145 transcripts that display "inter-sex" expression variations were defined as "Sexually dimorphic transcripts" (SDT), while 8,935 developmentally-regulated transcripts that do not exhibit sexual dimorphism were defined as "Non-sexually dimorphic transcripts" (NSDT).

Figure 2 Sexually dimorphic expression patterns during human gonad development.

(A) Heatmap representation of 13,145 SDTs, distributed into 14 expression patterns (P1 to P14), across seven developmental stages for both testes and ovaries. Each row corresponds to a transcript, and each column an experimental condition, *i.e.* the average of testes or ovaries from a given PCW. The standardized abundance of transcripts is color-coded according to the scale bar, red corresponding to the highest expression level, blue to the lowest. **(B)** Repartition of known markers involved in gonad differentiation and development within SDT expression patterns. Note that several isoforms of a given transcript can be assembled and display distinct expression. **(C)** Gene ontology (GO) terms found to be enriched (BH corrected p-value <0.05) in each expression pattern. **(D)** Transcript biotypes and isoform status proportion in SDT (pie chart) and within each cluster of differentially expressed transcripts (barplot). The comparison of the 13,145 SDT with the human reference transcriptome by Cuffcompare (Pollier *et al.*, 2013) classified them as known isoform (class code "="), novel isoforms (class code "j"), novel unannotated transcripts (NUTs) in intronic regions (class code "i"), intergenic

regions (“u”), antisense of known transcripts (class code “x”) or other ambiguous biotypes. Proportion of mRNAs, long non-coding (lnc)RNAs and NUTS in SDT clusters is given. Total number of transcripts in each cluster is indicated on the right side of the plot. An enrichment analysis using a hypergeometric strategy highlighted a significant accumulation of lncRNAs and NUT in the P12, P13 and P14 cluster (p-value <0.05) compared to their distribution within the 14 SDT clusters.

Figure 3 Non-sexually dimorphic expression patterns during human gonad development.

(A) Heatmap representation of 8,935 NSDTs, distributed into six expression patterns (Q1 to Q6), across seven developmental stages for both testes and ovaries. Each row is a transcript, and each column is an experimental condition, i.e. the average of testes or ovaries from a given PCW. The standardized abundance of transcripts is color-coded according to the scale bar, red corresponding to the highest expression level, blue to the lowest. **(B)** Repartition of known markers involved in gonad differentiation and development within SDT expression patterns. Note that several isoforms of a given can be assembled and display distinct expression. **(C)** GO terms found to be enriched (BH corrected p-value <0.05) in each expression pattern. **(D)** The comparison of the 8,935 NSDT with the human reference transcriptome by Cuffcompare (Pollier *et al.*, 2013) classified them as known isoform (class code “=”), novel isoforms (class code “j”), novel unannotaed transcripts (NUTs) in intronic regions (class code “i”), intergenic regions (“u”), antisense of known transcripts (class code “x”) or other ambiguous biotypes. Proportions of mRNAs, lncRNAs and NUTS in NSDT (pie chart) and within NSDT clusters are given (barplot). The total number of transcripts in each cluster is indicated on the right side of the barplot. An enrichment analysis using a hypergeometric strategy highlighted a significant accumulation of lncRNAs and NUTs in Q1 and Q6 clusters (p-value <0.05) compared to their distribution within the six NSDT clusters.

Figure 4 Cellular investigation of early-SDTs that are over-expressed in fetal testis.

Expression levels (line graphic) and quantitative RT-PCR (histograms) of genes from expression pattern P1 and P2, which exhibit a higher differential expression **(A)** at 6 PCW, such as sex determining region Y (*SRY*), wntless Wnt ligand secretion mediator (*WLS*), C-X-C motif chemokine ligand 14 (*CXCL14*) and C-C motif chemokine receptor 1 (*CCR1*), and **(B)** at 7 PCW, such as SRY-box 9 (*SOX9*), SRY-box 10 (*SOX10*), EPH receptor B1 (*EPHB1*), MAGE family member B1 (*MAGEB1*), fetal and adult testis expressed 1 (*FATE1*), erb-b2 receptor tyrosine kinase 3 (*ERBB3*), Cbp/p300 interacting transactivator with Glu/Asp rich carboxy-terminal domain 1 (*CITED1*) and novel unannotated transcript antisense of CITED1 (*TCONS_00249587*). Expression levels from RNA-sequencing (RNA-seq) as a function of age are depicted as blue lines for the testis and pink lines for the ovaries. Each point represents the mean fragments per kilobase of exon model per million reads mapped (FPKM) ± SEM of the levels measured in four (12 PCW and younger) and two different gonads (13-14 and 17 PCW). Quantitative PCR was performed on the different testicular sorted cell populations of germ cells (KIT+, red bars) Sertoli cells (hEpA+, green bars) and other cells (KIT-/ hEpA-, grey bars). Each column shows a pool of sorted cells from five fetal (6.9-7.3 PCW) testes. Each bar represents the mean ± SEM of the fold change in target gene expression relative to the reference genes *RPLP0* and *RPS20*. **(D)** Representative immunohistochemistry of SOX9, SOX10, KIAA1210, EPHB1, MAGEB1 and FATE1 on a 7.1 PCW testis. Arrows indicate germ cells (GC). Scale bar: 50 µM.

Figure 5 Cellular investigation of early-SDTs that are over-expressed in fetal ovary.

Expression levels (line graphic) and quantitative RT-PCR (histograms) of genes from expression pattern P8 and P9, which exhibit a higher differential expression **(A)** at 6 PCW, such as Neurexin 3 (*NRXN3*), contactin 1 (*CNTN1*) and SET nuclear proto-oncogene (*SET*), **(B)** at 7 PCW, such as R-spondin 1 (*RSPO1*), neuropeptide Y (*NPY*), SRY-box 4 (*SOX4*) and NUT *TCONS_00224470*, and **(C)** or later on, as POU class 5 homeobox 1 (*POU5F1*) and NUTs *TCONS_00113718, TCONS_00055038* and *TCONS_00042565*. Expression levels from RNA-seq as a function of age are depicted as blue lines for the testis and pink lines for the ovaries. Each point represents the mean FPKM ± SEM of the levels measured in four (12 PCW and younger) and two different gonads (13-14 and 17 PCW). Quantitative RT-PCR was performed on the ovarian sorted cell populations of germ cells (KIT+, pink bars) and other cells (KIT-, grey bars). Each column shows a pool of sorted cells from seven early differentiating (6.7-8.7 PCW, 7–9 PCW) and three fetal (10.6-11.7 PCW, 10–12 PCW) ovaries. Each bar represents the mean ± SEM of the fold change in target gene expression relative to the reference genes *RPLP0* and *RPS20*. **(D)** Immunofluorescence for NRXN3 (green) and KIT (red), LIN28 (green) and CNTN1 (red), and WT1 (green) and KIT (red), in early differentiating ovaries (6-6.6 PCW). Scale bar: 100 µM.

Supplementary Figure S1 Refinement strategy of assembled transcripts.

Following transcript reconstruction with Cufflinks, a refinement strategy was performed to discard sequencing and assembly artefacts: only transcripts with an expression of $\geqslant$ 1 FPKM in at least one experimental condition (average value of biological replicates) were considered; transcripts with a length of less than 200 nucleotides were discarded; novel transcript isoforms (Cuffcompare class “j”) and genes (classes “i”, “u” and “x”) were required to harbor at least two exons. FPKM = fragments per kilobase of exon model per million reads mapped.

Supplementary Figure S2 Genomic and expression features comparison.

Violin plot representation of selected expression and genomic features for all expressed mRNAs and long noncoding (lncRNAs) and novel unannotated transcripts (NUTs): **(A)** maximum abundance (log), **(B)** Shannon entropy, **(C)** sequence conservation (phastCons score), **(D)** cumulative exons size (log), **(E)** number of exons (log), and **(F)** GC content (%GC).

Supplementary Figure S3 Early sexually dimorphic expression patterns during human gonad development.

(A) Heatmap representation of 1,479 early sexually dimorphic transcripts (early-SDTs), distributed into 14 expression patterns (P1 to P14), across seven developmental stages for both testes and ovaries. Each row is a transcript, and each column is an experimental condition, i.e. the average of testes or ovaries from a given a gestational week (GW). The standardized abundance of transcripts is color-coded according to the scale bar, red corresponding to the highest expression level, blue to the lowest. **(B)** Repartition of known markers involved in gonad differentiation and development within early-SDT expression patterns. Note that several isoforms of a given gene can be assembled and display distinct expression. **(C)** Gene ontology (GO) terms found to be enriched (BH corrected p-value <0.05) in each expression pattern. **(D)** The comparison of the 1,479 early-SDT with the human reference transcriptome by Cuffcompare (Pollier *et al.*, 2013) classified them as known isoform (class code "="), novel isoforms (class code "j"), novel unannotated transcripts (NUTs) in intronic regions (class code "i"), intergenic regions ("u"), antisense of known transcripts (class code "x") or other ambiguous biotypes. Proportion of mRNAs, lncRNAs and NUTS in early-SDTs (pie chart) and within each cluster

is given (barplot). Total number of transcripts in each cluster is indicated on the right side of the barplot.

Supplementary Figure S4 Testicular and ovarian cell-sorting by flow cytometry.

(A) Representative immunofluorescence of hEpA-FITC (green) staining of cord cells and KIT-PE (red) staining of germ cells in testis sections of a 7 PCW old embryo. **(B)** Representative Side (SSC) versus Forward (FSC) scatter plot showing hEpA/Mast/stem cell growth factor receptor Kit (KIT) dot plots according to size (FSC-H) and cellular granularity (SSC-H). Example of gating strategy for flow cytometry sorting of Sertoli cells (hEpA+/KIT-, green dots), germ cells (hEpA-/KIT+, red plots) and other cells types (hEpA-/KIT-, grey plots). **(C)** Quantitative RT-PCR of KIT proto-oncogene, receptor tyrosine kinase (KIT), nuclear receptor subfamily 2 group F member 2 (NR2F2)and SRY-box transcription factor 9 (SOX9) was performed on the different sorted cell populations of germ cells (KIT+, red bars) Sertoli cells (hEpA+, green bars) and other cells (KIT-/ hEpA-, grey bars). Each column shows a pool of sorted cells from five fetal (6.9-7.3 PCW) testes. Each bar represents the mean ± SEM of the fold change in target gene expression relative to the reference genes ribosomal protein lateral stalk subunit P0 (RPLP0) and ribosomal protein S20 (RPS20). **(D)** Representative immunofluorescence of KIT-PE (red) staining of germ cells in sections of an ovary at 11 PCW. **(E)** SSC versus FSC scatter plot showing KIT dot plots according to size (FSC-H) and cellular granularity (SSC-H). Example of gating strategy for flow cytometry sorting of germ cells (KIT+, red plots) and other cells types (KIT-, grey plots). **(F)** Quantitative RT-PCR of KIT, NR2F2 and forkhead box L2 (FOXL2) was performed on the different sorted cell populations of germ cells (KIT+, red bars) and other cells (KIT-, grey bars). Each column shows a pool of sorted cells from seven early differentiating (6.7-8.7 PCW, 7–9 PCW) and three fetal (10.6-11.7 PCW, 10–12 PCW) ovaries. Each bar represents

285 the mean ± SEM of the fold change in target gene expression relative to the reference genes RPLP0
286 and RPS20. Scale bars: 100 µM.

287

288 Table legends

289 **Table I. List of primers that were used for q-PCR experiments.**

290 **Table II. Antibodies used for immunofluorescence and immunohistochemistry.**

291 **Supplementary Table SI. Statistics for read mapping and transcript assembly.**

292 **Supplementary Table SII. Early sexually dimorphic transcripts encoding transcription factors.**

Table I List of primers that were used for quantitative PCR experiments.

Gene	Forward (5'-3')
CCR1	CAGAAAGCCCCAGAAACAAA
CITED1	TGCACTTGATGTCAAGGGTG
CNTN1	TTGGGAAGATGGTAGCTTGG
CXCL14	ATGAAGCCAAAGTACCCGCA
EPHB1	AGAGGAGGGAAAAGGACCAGG
ERBB3	ACAGCCCCAGATCTGCAC
FATE1	GGCAATTTCCAAGGCATACG
FOXL2	GCGAAGTTCCCGTTCTACGA
KIT	TTCTTACCAGGTGGCAAAGG
MAGEB1	CTATGGGGAACCCCGTAAGT
NPY	CTACATCAACCTCATCACCAGG
NR2F2	GCCATAGTCCTGTTCACCTCA
NRXN3	GCTGAGAACAACCCCAATA
POU5F1	TACTCCTCGGTCCCTTTCC
RPLP0	TCTACAACCCTGAAGTGCTTGAT
RPS20	AACAAGCCGCAACGTAAAATC
RSPO1	ACACTTCCCAGCATCTGAGACCAA
SET	AAATCAAATGGAAATCTGGAAAGG
SOX10	AAGCCTCACATCGACTTCGG
SOX4	GACCTGCTCGACCTGAACC
SOX9	AACGCCTTCATGGTGTGG
SRY	ACAGTAAAGGCAACGTCCAG
TCONS_00042565	GCGGCCCTAAGACAAAGAAC
TCONS_00055038	CCCACCTTCCTCCTTCCTG
TCONS_00113718	GCCCAACCACAGAAGGTTT
TCONS_00153406	TCTACTTGTTTCTGGAGCTGAAG
TCONS_00224470	CCTGGGCTACACTGGTCTTT
TCONS_00249587	GGGAGAAAAGTAGCCCCAAG
WLS	CCTTGGTTCCAATTCATGCT

Reverse (5’-3’)	Size (bp)	Reference
GGTGTTTGGAGTTTCCATCC	80	Primer 3
GTTGTAGGAGAGCCTATTGG	201	PMID:22703800
TGATAACAAGGGTTCCAGTGC	116	PMID: 26855587
TCTCGTTCCAGGCGTTGTAC	148	PMID: 24700803
GGTTTCCCACGGCATCTC	183	PMID: 24121831
GTTGGGCGAATGTTCTCATC	78	PMID: 23991224
CTAGTCTGCGCCACTGCATC	68	PMID: 17761949
CTCGTTGAGGCTGAGGTTGT	75	Primer BLAST
AAATGCTTTCAGGTGCCATC	209	PMID: 21668453
GGTTTCAGCATAGGCTCTCG	130	Primer 3
TCACCACATTGCAGGGTCT	133	PMID: 27722841
AATCTCGTCGGCTGGTTG	131	PMID: 24318875
ATGCTGGCTGTAGAGCGATT	179	PMID: 28013231
CAAAAACCCTGGCACAAACT	131	PMID: 24743772
CAATCTGCAGACAGACACTGG	96	PMID: 24743772
ACGATCCCACGTCTTAGAACC	166	PMID: 24743772
TGCTGAACAGGATGGGAAGAAGGT	146	PMID: 23617070
AAAGAAGCTCTCTGGTTCCTCATG	101	PMID: 22677993
TCCATGTTGGACATTACCTCGT	67	PMID: 23338937
CCGGGCTCGAAGTTAAAATCC	107	PMID: 28535514
TCTCGCTCTCGTTCAGAAGTC	124	Primer3
ATCTGCGGGAAGCAAACTGC	293	PMID: 11869379
TCTGACCAGAAAATCGCTTC	104	Primer3
TCAGTGCAGAAGAGCCCAA	86	Primer3
CTGGGACAGGATGGAGAGG	97	Primer3
TGCAGTAACATCCTCCTCCTC	120	Primer3
GAGCACCTCATTCTTGGCT	70	Primer3
GAAGCAAATGGAGAGACGGA	111	Primer 3
TTCAGTCCACTCAGCAAACG	138	Primer3

Table II Antibodies used for immunofluorescence and immunohistochemistry.

Antigen		**Heat Induced Epitope Retrieval**
hEpA-FITC	Mouse FITC-coupled anti-human epithelial antigen	-
CNTN1	Contactin 1	Citrate
EPHB1	ephrin type-B receptor 1	Citrate
ERBB3	HER3/ErbB3 (D22C5) XP® Rabbit mAb	Citrate
FATE1	fetal and adult testis expressed 1	Citrate
KIAA1210	KIAA1210	Citrate
KIT/CD117-PE	mouse R-Phycoerythrin-coupled anti-human KIT/CD117; clone 104D2	-
LIN28	lin-28 homolog A	Citrate
MAGEB1	melanoma-associated antigen B1	Citrate
NRXN3	neurexin 3	Citrate
SOX9	SRY (sex determining region Y)-box9	Citrate
SOX10	SRY (sex determining region Y)-box 10	Citrate
WT1	Wilms tumor 1	Citrate

Dilution	Antibody supplier and product number
1 :100	Dako, F0860
1 :100 (IF)	R&D systems, AF904
1:2500- 1:5000	Sigma, HPA067740
0.215277778	Cell Signaling Tech., #12708
1:1000-1:2500	Sigma, HPA034604
1:200- 1:500	Sigma, HPA048322
1 :100	BioLegend, 313204
1 :100 (IF)	Abcam, Ab46020
1:100 - 1:250	Sigma, HPA001193
1 :200 / 1 :100 (IF)	Sigma, HPA0002727
0.111111111	Millipore, AB5535
1:200- 1:500	Sigma, HPA068898
1:100 (IF)	Santa-Cruz Biotech, sc-192

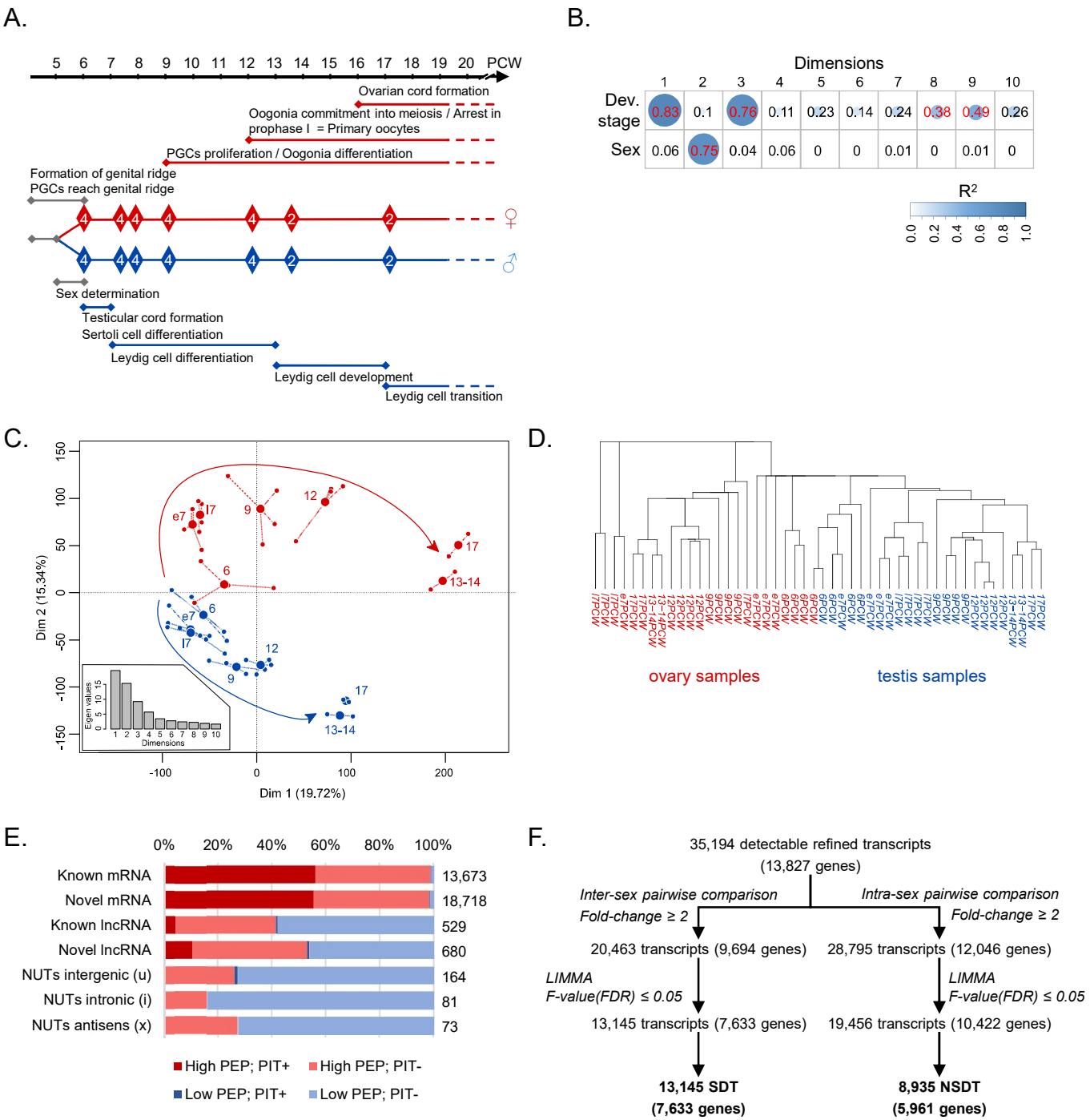
A.
5 6 7 8 9 10 11 12 13 14 15 16 17 18 19 20 PCW
Ovarian cord formation
Oogonia commitment into meiosis / Arrest in prophase I = Primary oocytes
PGCs proliferation / Oogonia differentiation
Formation of genital ridge
PGCs reach genital ridge
Sex determination
Testicular cord formation
Sertoli cell differentiation
Leydig cell differentiation
Leydig cell development
Leydig cell transition
B.
Dimensions
1 2 3 4 5 6 7 8 9 10
Dev. stage 0.83 0.1 0.76 0.11 0.23 0.14 0.24 0.38 0.49 0.26
Sex 0.06 0.75 0.04 0.06 0 0 0.01 0 0.01 0
R²
0.0 0.2 0.4 0.6 0.8 1.0
C.
Dim 2 (15.34%)
Dim 1 (19.72%)
Eigen values
Dimensions
D.
ovary samples
testis samples
E.
0% 20% 40% 60% 80% 100%
Known mRNA 13,673
Novel mRNA 18,718
Known lncRNA 529
Novel lncRNA 680
NUTs intergenic (u) 164
NUTs intronic (i) 81
NUTs antisens (x) 73
High PEP; PIT+
High PEP; PIT-
Low PEP; PIT+
Low PEP; PIT-
F.
35,194 detectable refined transcripts
(13,827 genes)
Inter-sex pairwise comparison
Fold-change ≥ 2
Intra-sex pairwise comparison
Fold-change ≥ 2
20,463 transcripts (9,694 genes)
28,795 transcripts (12,046 genes)
LIMMA
F-value(FDR) ≤ 0.05
LIMMA
F-value(FDR) ≤ 0.05
13,145 transcripts (7,633 genes)
19,456 transcripts (10,422 genes)
13,145 SDT
(7,633 genes)
8,935 NSDT
(5,961 genes)

Fig. 1

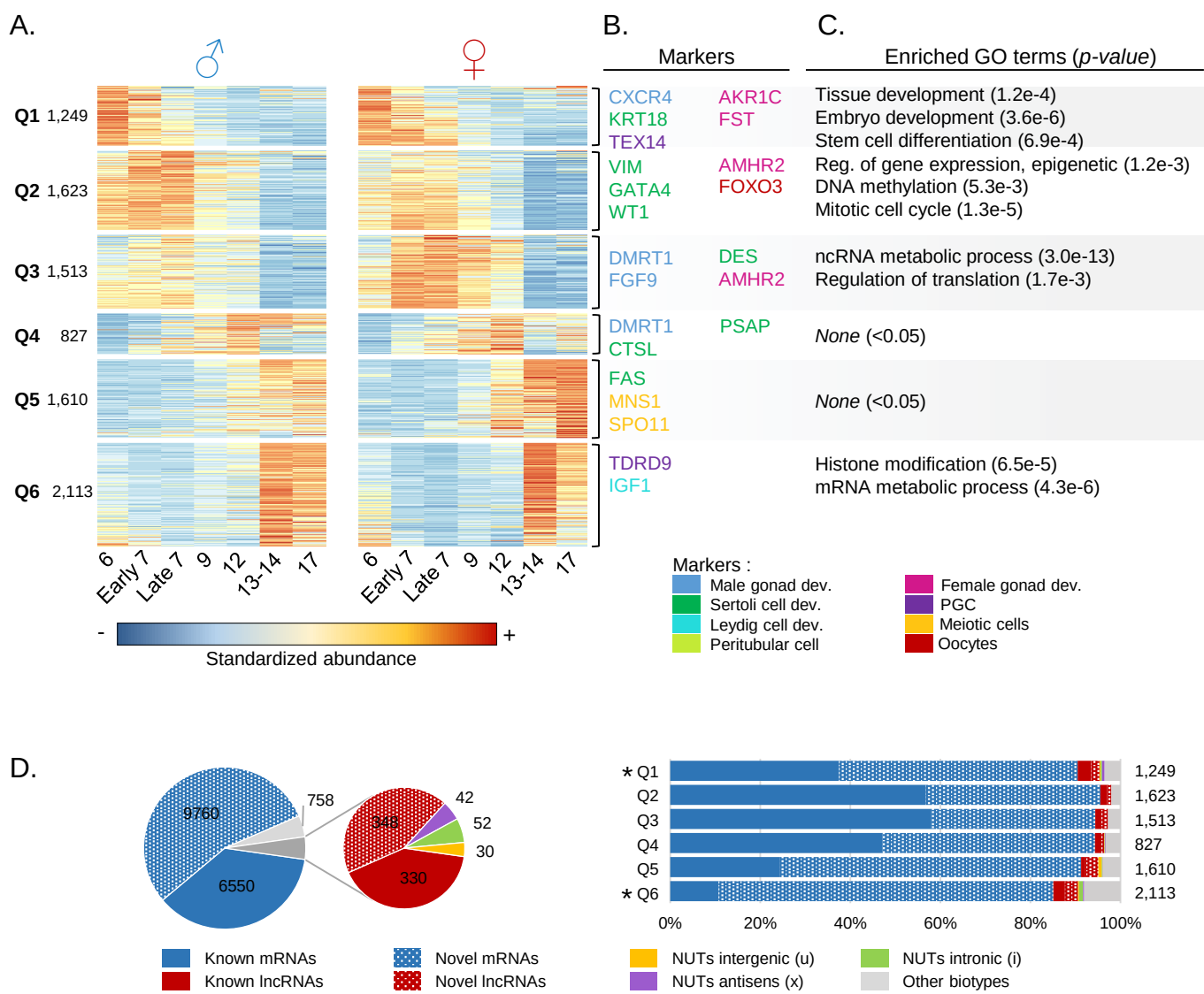
A.
B.
C.
Markers
Enriched GO terms (p-value)
Q1 1,249
Q2 1,623
Q3 1,513
Q4 827
Q5 1,610
Q6 2,113
CXCR4
KRT18
TEX14
AKR1C
FST
Tissue development (1.2e-4)
Embryo development (3.6e-6)
Stem cell differentiation (6.9e-4)
VIM
GATA4
WT1
AMHR2
FOXO3
Reg. of gene expression, epigenetic (1.2e-3)
DNA methylation (5.3e-3)
Mitotic cell cycle (1.3e-5)
DMRT1
FGF9
DES
AMHR2
ncRNA metabolic process (3.0e-13)
Regulation of translation (1.7e-3)
DMRT1
CTSL
PSAP
None (<0.05)
FAS
MNS1
SPO11
None (<0.05)
TDRD9
IGF1
Histone modification (6.5e-5)
mRNA metabolic process (4.3e-6)
6
Early 7
Late 7
9
12
13-14
17
Standardized abundance
Markers :
Male gonad dev.
Sertoli cell dev.
Leydig cell dev.
Peritubular cell
Female gonad dev.
PGC
Meiotic cells
Oocytes
D.
9760
758
6550
348
42
52
30
330
Known mRNAs
Known lncRNAs
Novel mRNAs
Novel lncRNAs
* Q1
Q2
Q3
Q4
Q5
* Q6
1,249
1,623
1,513
827
1,610
2,113
0%
20%
40%
60%
80%
100%
NUTs intergenic (u)
NUTs antisens (x)
NUTs intronic (i)
Other biotypes

Fig. 3

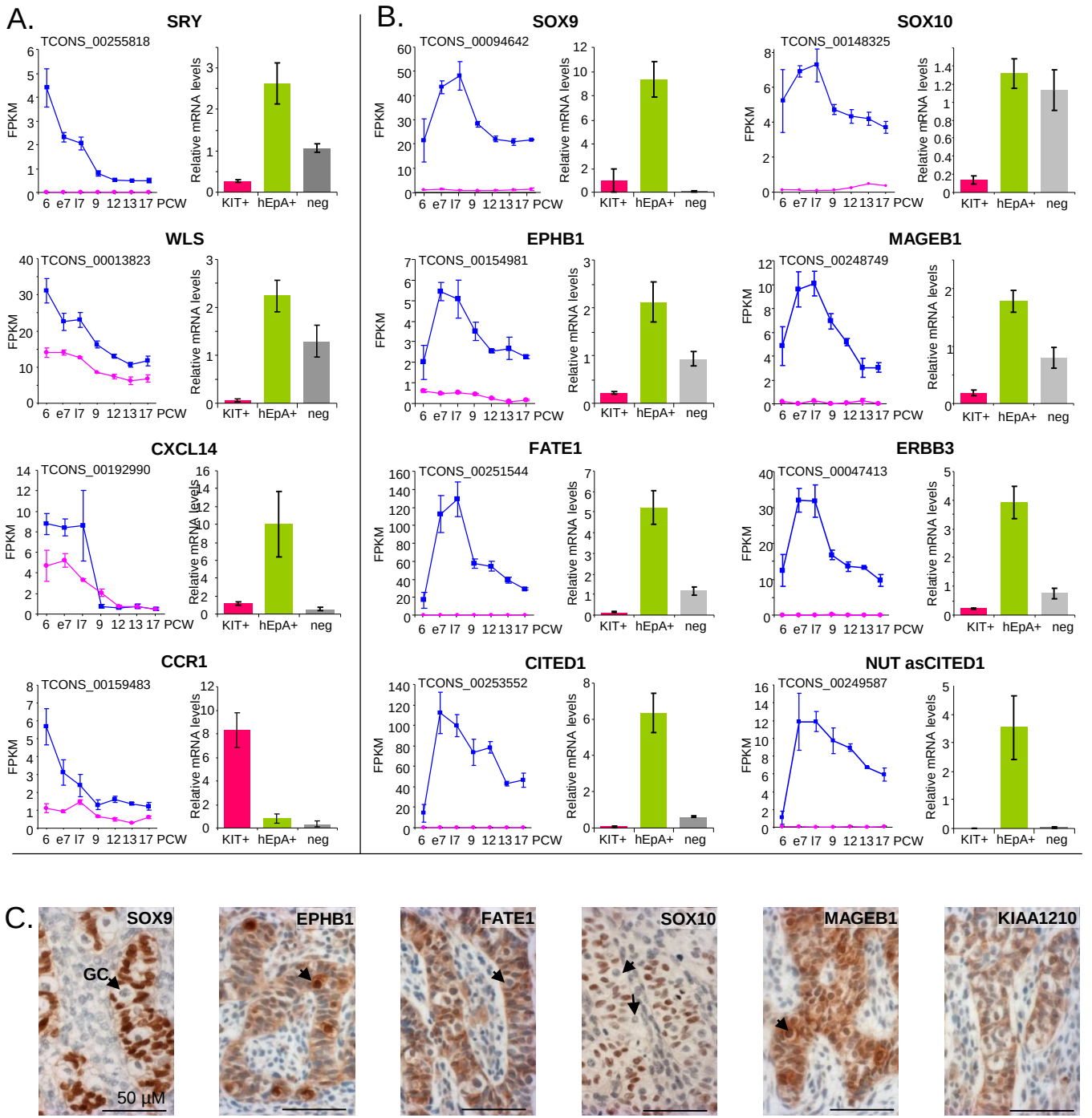
A.
SRY
TCONS_00255818
WLS
TCONS_00013823
CXCL14
TCONS_00192990
CCR1
TCONS_00159483
B.
SOX9
TCONS_00094642
SOX10
TCONS_00148325
EPHB1
TCONS_00154981
MAGEB1
TCONS_00248749
FATE1
TCONS_00251544
ERBB3
TCONS_00047413
CITED1
TCONS_00253552
NUT asCITED1
TCONS_00249587
FPKM
Relative mRNA levels
6 e7 l7 9 12 13 17 PCW
KIT+ hEpA+ neg

C.
SOX9
GC
50 μM
EPHB1
FATE1
SOX10
MAGEB1
KIAA1210

Fig. 4

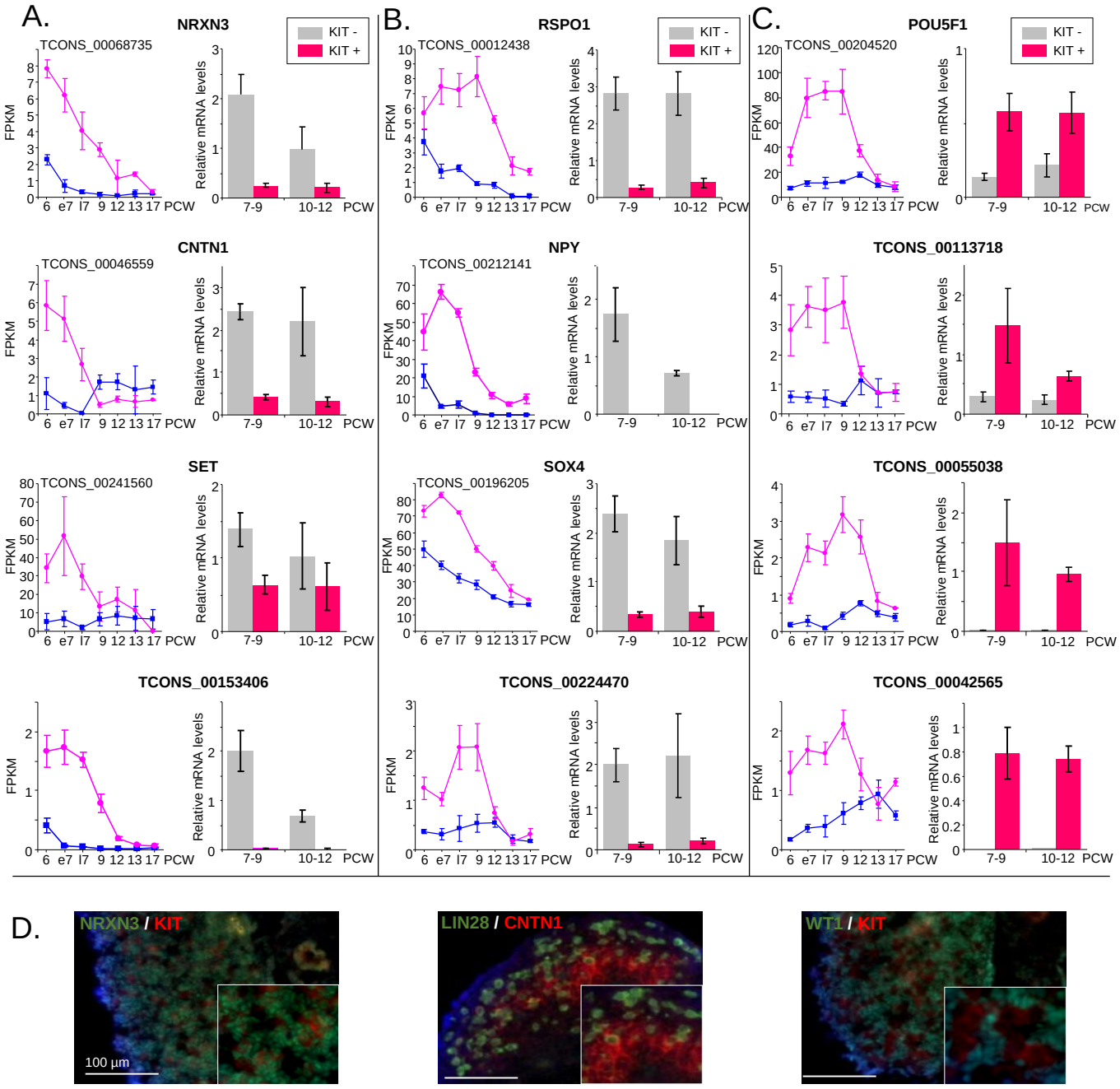
A.
NRXN3
TCONS_00068735
CNTN1
TCONS_00046559
SET
TCONS_00241560
TCONS_00153406
B.
RSPO1
TCONS_00012438
NPY
TCONS_00212141
SOX4
TCONS_00196205
TCONS_00224470
C.
POU5F1
TCONS_00204520
TCONS_00113718
TCONS_00055038
TCONS_00042565
KIT -
KIT +
FPKM
Relative mRNA levels
6 e7 l7 9 12 13 17 PCW
7-9
10-12 PCW

D.
NRXN3 / KIT
100 µm
LIN28 / CNTN1
WT1 / KIT

Fig. 5

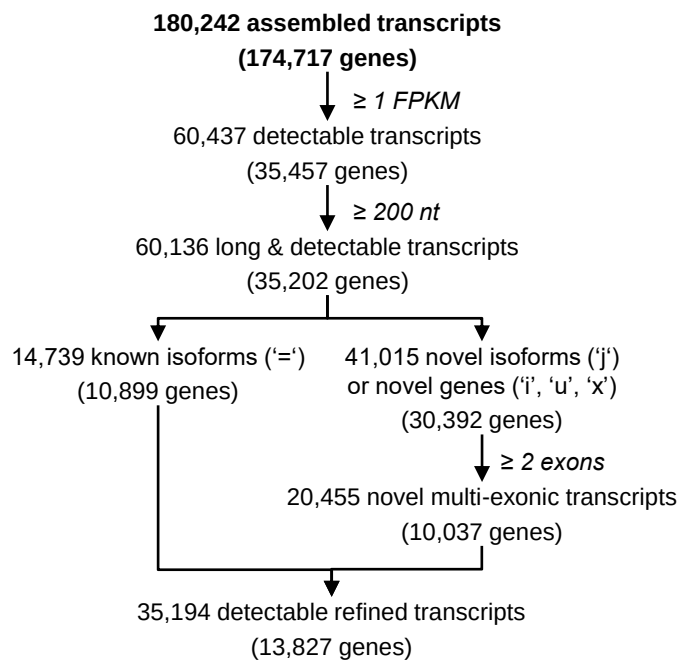
180,242 assembled transcripts
(174,717 genes)
≥ 1 FPKM
60,437 detectable transcripts
(35,457 genes)
≥ 200 nt
60,136 long & detectable transcripts
(35,202 genes)
14,739 known isoforms (‘=‘)
(10,899 genes)
41,015 novel isoforms (‘j‘)
or novel genes (‘i’, ‘u’, ‘x’)
(30,392 genes)
≥ 2 exons
20,455 novel multi-exonic transcripts
(10,037 genes)
35,194 detectable refined transcripts
(13,827 genes)

Fig. S1

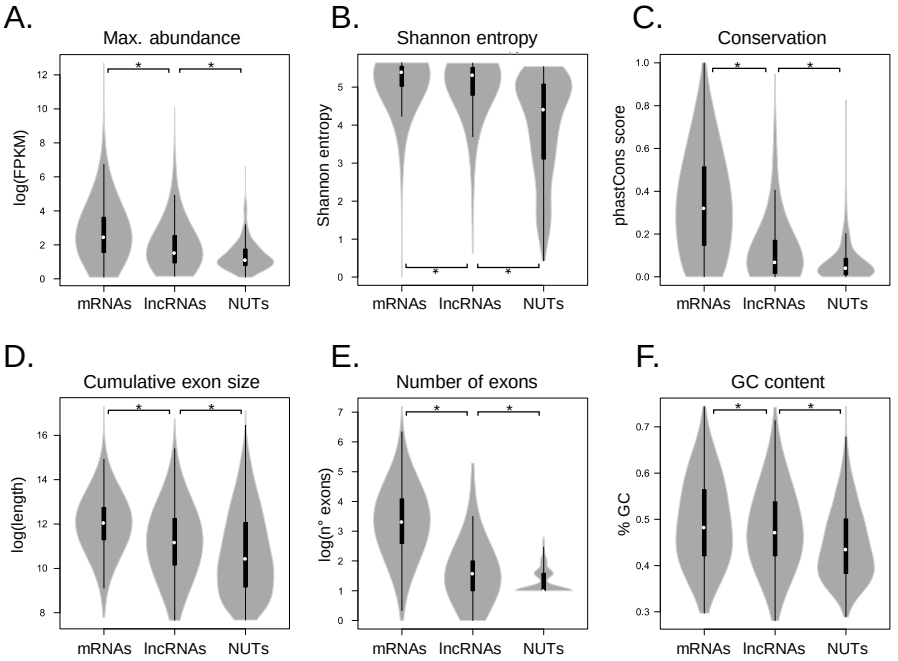
A.
Max. abundance
log(FPKM)
mRNAs
lncRNAs
NUTs
B.
Shannon entropy
Shannon entropy
C.
Conservation
phastCons score
D.
Cumulative exon size
log(length)
E.
Number of exons
log(n° exons)
F.
GC content
% GC

Fig. S2

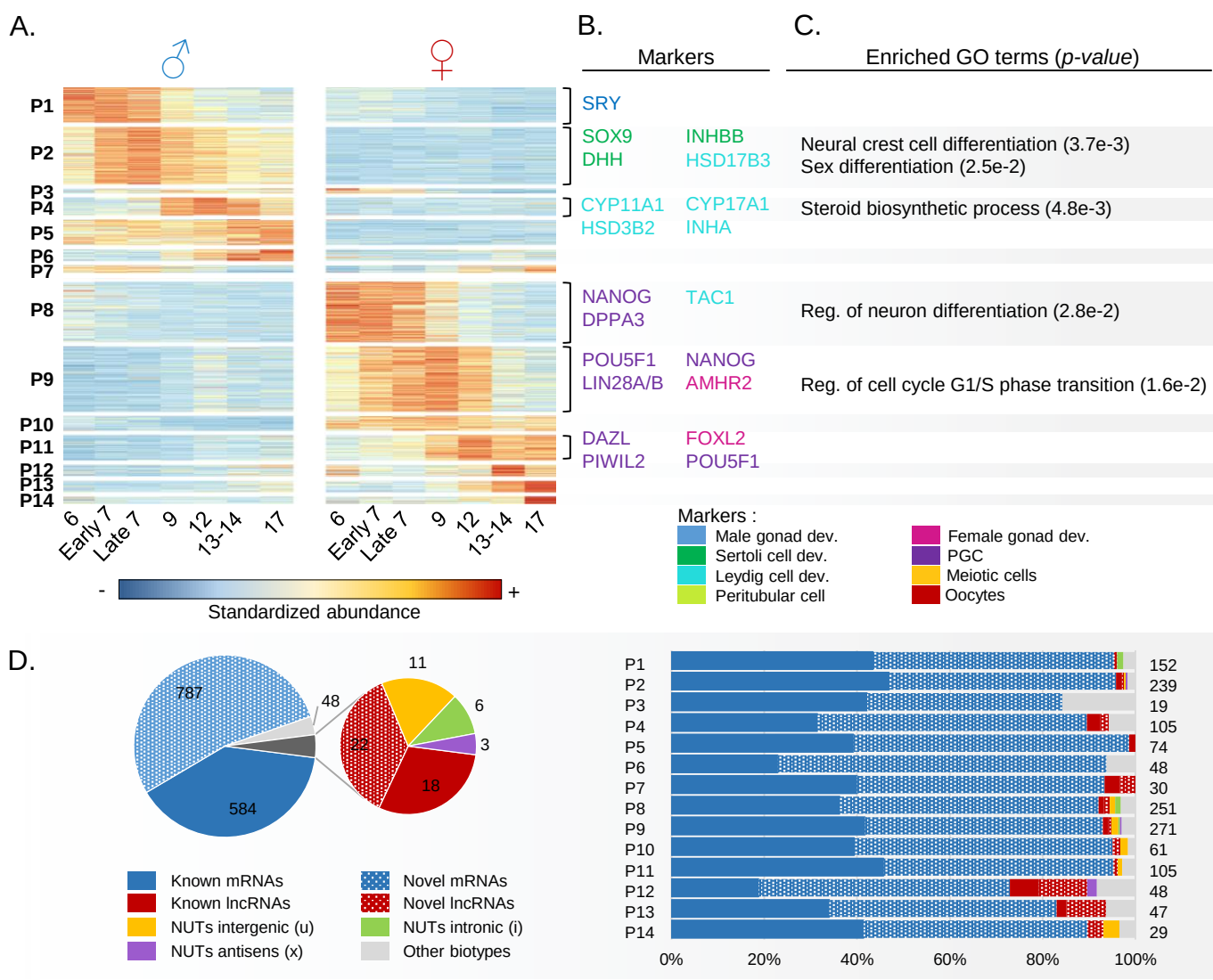
A.
B.
C.
Markers
Enriched GO terms (p-value)
P1
P2
P3
P4
P5
P6
P7
P8
P9
P10
P11
P12
P13
P14
SRY
SOX9
DHH
INHBB
HSD17B3
Neural crest cell differentiation (3.7e-3)
Sex differentiation (2.5e-2)
CYP11A1
HSD3B2
CYP17A1
INHA
Steroid biosynthetic process (4.8e-3)
NANOG
DPPA3
TAC1
Reg. of neuron differentiation (2.8e-2)
POU5F1
LIN28A/B
NANOG
AMHR2
Reg. of cell cycle G1/S phase transition (1.6e-2)
DAZL
PIWIL2
FOXL2
POU5F1
6
Early 7
Late 7
9
12
13-14
17
Standardized abundance
Markers :
Male gonad dev.
Sertoli cell dev.
Leydig cell dev.
Peritubular cell
Female gonad dev.
PGC
Meiotic cells
Oocytes

D.
787
584
48
11
6
3
22
18
Known mRNAs
Known lncRNAs
NUTs intergenic (u)
NUTs antisens (x)
Novel mRNAs
Novel lncRNAs
NUTs intronic (i)
Other biotypes
P1 152
P2 239
P3 19
P4 105
P5 74
P6 48
P7 30
P8 251
P9 271
P10 61
P11 105
P12 48
P13 47
P14 29
0%
20%
40%
60%
80%
100%

Fig. S3

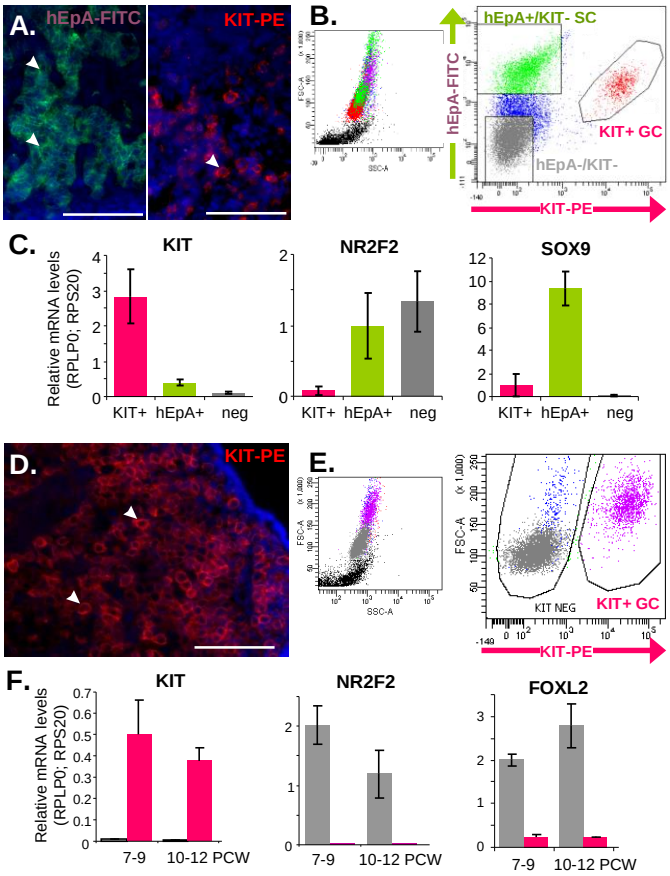
A.
hEpA-FITC
KIT-PE
B.
hEpA+/KIT- SC
hEpA-FITC
KIT+ GC
hEpA-/KIT-
KIT-PE
C.
KIT
NR2F2
SOX9
Relative mRNA levels (RPLP0; RPS20)
KIT+ hEpA+ neg
D.
KIT-PE
E.
FSC-A
SSC-A
KIT NEG
KIT+ GC
KIT-PE
F.
KIT
NR2F2
FOXL2
Relative mRNA levels (RPLP0; RPS20)
7-9 10-12 PCW

Fig. S4

Supplementary Table SI Statistics for read mapping and transcript assembly.

Average number of raw and mapped reads, percentage of mapping and number of assembled transcripts are indicate
PCW = post conceptional week. The number of non-redundant assembled transcripts is also provided during testicul
as the overall number of non-redundant assembled transcripts in this study.

	PCW	6	e7	l7	9	12
Fetal testis	n° samples	4	4	4	4	4
	Average sequenced pairs of read	50,163,366 +- 5 540 241	43,637,558 +- 3 217 370	45,033,799 +- 4 891 256	44,578,922 -6124741	61,408,394 +- 31 392 665
	Average mapped pairs of read	45,088,608 +- 4 567 496	39,066,943 +-2 877 937	38,915,843 +- 6 718 006	36,500,690 +- 3 675 842	46,586,645 +- 20 642 653
	% of mapped reads	89.9	89.5	86.4	81.9	75.9
	n° reconstructed transcripts	164,931	129,802	103,431	116,903	107,148
Fetal ovary	n° samples	4	4	4	4	4
	Average sequenced pairs of read	51,756,993 +- 3 476 980	42,038,738 +- 3 950 805	43,167,327 +- 6 221 180	45,461,320 +- 8 410 709	43,085,238 +- 6 565 924
	Average mapped pairs of read	46,047,326 +- 3 200 842	38,087,267 +-3 581 721	33,349,134 +- 3 167 555	37,688,289 +- 10 017 251	34,516,893 +- 5 232 477
	% of mapped reads	89	90.6	77.3	82.9	80.1
	n° recontructed transcripts	186,499	121,800	93,201	12,817	112,165
						n° of non-redundant

d for each experimental condition.
ar and ovarian developments, as well

13-14	17	Total
2	2	24
46,992,435 +-3 747 882	47,295,757 +- 2 131 643	339,110,230
40,120,429 +- 2 994 901	38,721,188 +- 4 093 627	285,000,344
85.4	81.9	84.4
164,652	147,287	142,953
2	2	24
47,163,616 +- 3 195 188	38,044,232 +- 2 869 127	310,717,463
38,186,847 +- 1 789 162	33,236,072 +- 2 927 283	261,111,827
81	87.4	84
191,983	174,783	168,195
reconstructed transcripts		**180,242**

Supplementary Table SII Early sexually dimorph
Early sexually dimorphic transcripts (eSDT) corresp
pattern(s) (column D) and their early SDT target ge
target genes were extracted from public databases ir
2012). Gene names in red, green or blue have know

Gene symbol	Ensemble Gene IDs
ADAMTS19	ENSG00000145808
BACH2	ENSG00000112182
BCL11B	ENSG00000127152
BIN1	ENSG00000136717
BRDT	ENSG00000137948
BRIP1	ENSG00000136492
CBFA2T2	ENSG00000078699
CDX1	ENSG00000113722
CDYL	ENSG00000153046
CHD9	ENSG00000177200
CITED1	ENSG00000125931
CREBBP	ENSG00000005339
CREM	ENSG00000095794
CUL4B	ENSG00000158290
CUX2	ENSG00000111249
DEPDC7	ENSG00000121690
ELF4	ENSG00000102034
ESR1	ENSG00000091831
ESR2	ENSG00000140009
ETV4	ENSG00000175832
ETV5	ENSG00000244405
FOSL2	ENSG00000075426
FOXH1	ENSG00000160973
FOXI3	ENSG00000214336
FOXL2	ENSG00000183770
GABPB2	ENSG00000143458
GATAD2A	ENSG00000167491
GLI1	ENSG00000111087
GRIP1	ENSG00000155974
HEY2	ENSG00000135547
HIC2	ENSG00000169635
HIST1H1T	ENSG00000187475
HIVEP2	ENSG00000010818
IRX1	ENSG00000170549
KDM4C	ENSG00000107077
KLF16	ENSG00000129911
KLF4	ENSG00000136826
KLF8	ENSG00000102349
LARP1B	ENSG00000138709

LBX2	ENSG00000179528
LHX2	ENSG00000106689
LHX9	ENSG00000143355
LIN28A	ENSG00000131914
LIN28B	ENSG00000187772
MACF1	ENSG00000127603
MAEL	ENSG00000143194
MBNL2	ENSG00000139793
MED23	ENSG00000112282
MTA1	ENSG00000182979
MYBL2	ENSG00000101057
MYCL	ENSG00000116990
NANOG	ENSG00000111704
NANOGP1	ENSG00000176654
NCOA1	ENSG00000084676
NCOR1	ENSG00000141027
NFAT5	ENSG00000102908
NFATC2	ENSG00000101096
NFE2L3	ENSG00000050344
NFKB2	ENSG00000077150
NKRF	ENSG00000186416
NKX3-1	ENSG00000167034
NR6A1	ENSG00000148200
NRG1	ENSG00000157168
NRK	ENSG00000123572
ONECUT1	ENSG00000169856
PHB2	ENSG00000215021
PHF8	ENSG00000172943
PLXNC1	ENSG00000136040
POU5F1	ENSG00000204531
POU5F1B	ENSG00000212993
PPARG	ENSG00000132170
PRDM1	ENSG00000057657
RAD51	ENSG00000051180
RBM26	ENSG00000139746
RBMX	ENSG00000147274
REST	ENSG00000084093
RFX2	ENSG00000087903
RNF125	ENSG00000101695
RP11-313J2.1	ENSG00000215146
SALL1	ENSG00000103449
SALL4	ENSG00000101115
SAMD11	ENSG00000187634
SAP18	ENSG00000150459
SETDB2	ENSG00000136169
SF3A2	ENSG00000104897
SMAD9	ENSG00000120693
SMARCA1	ENSG00000102038

SOX10	ENSG00000100146
SOX9	ENSG00000125398
SP6	ENSG00000189120
SRY	ENSG00000184895
TBX1	ENSG00000184058
TCF25	ENSG00000141002
TCF3	ENSG00000071564
TEAD4	ENSG00000197905
TFAP2C	ENSG00000087510
TOX	ENSG00000198846
UBTF	ENSG00000108312
VENTX	ENSG00000151650
WHSC1	ENSG00000109685
ZBTB1	ENSG00000126804
ZBTB7C	ENSG00000184828
ZC3H11A	ENSG00000058673
ZC3HAV1	ENSG00000105939
ZFP30	ENSG00000120784
ZFP42	ENSG00000179059
ZFY	ENSG00000067646
ZFYVE20	ENSG00000131381
ZKSCAN8	ENSG00000198315
ZMYND11	ENSG00000015171
ZMYND8	ENSG00000101040
ZNF138	ENSG00000197008
ZNF208	ENSG00000160321
ZNF213	ENSG00000085644
ZNF217	ENSG00000171940
ZNF227	ENSG00000131115
ZNF232	ENSG00000167840
ZNF281	ENSG00000162702
ZNF385A	ENSG00000161642
ZNF41	ENSG00000147124
ZNF468	ENSG00000204604
ZNF560	ENSG00000198028
ZNF607	ENSG00000198182
ZNF638	ENSG00000075292
ZNF66	ENSG00000160229
ZNF676	ENSG00000196109
ZNF729	ENSG00000196350
ZNF76	ENSG00000065029
ZNF90	ENSG00000213988
ZNF93	ENSG00000184635
ZNF98	ENSG00000197360

ıic transcripts encoding transcription factors in human.
ɔonding to genes encoding transcription factors (columns A-C), their corresponding expression
ıes (column E) are reported. Known interactions between transcription factors and their known
ıcluding TRRUST (Han *et al.* , 2015) and the Transcription Factor encyclopedia (Yusuf *et al.* ,
n associations with sex reversal, disorders of sexual development or testis/ovary cancer, respectively.

Assembled transcripts IDs	**Expression patterns**	**eSDT target genes**
TCONS_00184938	P8	-
TCONS_00206773;TCONS_00206776;TCONS_00206777	P8	-
TCONS_00073504	P8	-
TCONS_00130031;TCONS_00130033	P9	-
TCONS_00004335	P14	-
TCONS_00098944	P7	-
TCONS_00136955	P9	-
TCONS_00185901	P11	**PPARG**;POSTN
TCONS_00195284	P8	-
TCONS_00084978	P3	-
TCONS_00249587;TCONS_00253552;TCONS_00253553;TCONS_00253554;TCONS_00253556	P2	-
TCONS_00087391	P11	RAD51
TCONS_00022167	P1	ACE;TAC1;G6PD
TCONS_00254445;TCONS_00254446	P1	-
TCONS_00049582	P8	-
TCONS_00033456	P11	-
TCONS_00254729	P5	-
TCONS_00201882	P12	PMAIP1;GREB1;ESR1;PLAC1
TCONS_00072230	P11	-
TCONS_00097882;TCONS_00097883	P9	-
TCONS_00165043	P9	-
TCONS_00115256	P6	CLU
TCONS_00236474	P9	-
TCONS_00128881	P9	-
TCONS_00163150	P11	FOXL2;**CYP17A1**;**CYP11A1**
TCONS_00005817	P13	-
TCONS_00107359;TCONS_00107362	P9	-
TCONS_00047499	P2	**SOX9**;SFRP1
TCONS_00053783	P8	-
TCONS_00200804	P2	-
TCONS_00145356;TCONS_00145358	P9	-
TCONS_00204095	P13	-
TCONS_00208943	P5	-
TCONS_00180488;TCONS_00180489	P8	-
TCONS_00237196	P12	-
TCONS_00110133	P8	-
TCONS_00245945	P9	LAMA3;LAMA1;NANOG;PFKP;IFITM3
TCONS_00249352	P9	-
TCONS_00170683	P9	-

TCONS_00128298	P8	-
TCONS_00241252	P11	-
TCONS_00007929	P6	-
TCONS_00001570;TCONS_00001571	P9	-
TCONS_00199732	P9	-
TCONS_00002167	P11	-
TCONS_00006676	P13	-
TCONS_00060407	P2	-
TCONS_00208410	P9	-
TCONS_00070138	P13	ESR1
TCONS_00137452	P9	MYBL2
TCONS_00012583;TCONS_00012585	P9	-
TCONS_00044962;TCONS_00044963	P8;P9	POU5F1
TCONS_00044969	P9	-
TCONS_00115064	P11	-
TCONS_00096460;TCONS_00096465	P5;P1	**PPARG**;IGFBP3;ESR1
TCONS_00085918	P7	CCL2
TCONS_00140516;TCONS_00140524	P8	ENPP2
TCONS_00212178	P9	-
TCONS_00024595	P2	-
TCONS_00254399	P8	-
TCONS_00232099;TCONS_00232101	P5;P2	ESR1;**ACTG2**
TCONS_00246680;TCONS_00246681	P11	-
TCONS_00226393	P8	-
TCONS_00250221	P8	-
TCONS_00080027	P8	-
TCONS_00051081	P2	-
TCONS_00253265	P13	-
TCONS_00048895	P2	-
TCONS_00204519;TCONS_00204520	P9	NANOG;**ZFP42**
TCONS_00230146	P9	-
TCONS_00149760	P9	CAV1;KLF4;GSTA2
TCONS_00199766;TCONS_00199790	P9	-
TCONS_00075018	P8	-
TCONS_00063928	P1	-
TCONS_00254939	P12	**KIT**
TCONS_00168163;TCONS_00168164	P8	TAC1;LIN28A;GABRB3;KCNQ2
TCONS_00110433	P13	-
TCONS_00101424	P9	-
TCONS_00027617	P9	-
TCONS_00088597	P10	-
TCONS_00140537;TCONS_00140540;TCONS_00140543;TCONS_00140544	P9	SALL4;POU5F1
TCONS_00000033;TCONS_00000037	P1	-
TCONS_00056892	P8	-
TCONS_00058144;TCONS_00058145;TCONS_00058146	P8	-
TCONS_00106327;TCONS_00106328;TCONS_00106329	P2;P5	-
TCONS_00061933	P7	-
TCONS_00254705	P2	-

TCONS_00148324;TCONS_00148325	P2	MPZ;PLP1;GJB1;**EDNRB**
TCONS_00094642	P2	KLF4;COL2A1;HAPLN1;COL9A1;PRAME;**SOX10**
TCONS_00098228	P1	-
TCONS_00255818	P1	**SOX9**;**PROM1**
TCONS_00145221	P2	-
TCONS_00086893;TCONS_00086894	P2	-
TCONS_00110107;TCONS_00110108;TCONS_00110111	P13;P9	POU5F1
TCONS_00044600	P9	-
TCONS_00137982;TCONS_00137983	P9	ESR1
TCONS_00233028	P5	-
TCONS_00097957	P8	-
TCONS_00025976	P8	-
TCONS_00166063	P9	-
TCONS_00067741	P1	-
TCONS_00104942	P2	-
TCONS_00008281	P6	-
TCONS_00223757	P3	-
TCONS_00112190	P12	-
TCONS_00173057;TCONS_00173058;TCONS_00173059	P8;P9	-
TCONS_00255507;TCONS_00255508;TCONS_00255510	P2;P5	-
TCONS_00158407	P3	-
TCONS_00196743	P10	-
TCONS_00020765	P14	-
TCONS_00140371	P4	-
TCONS_00213671	P8	-
TCONS_00111586;TCONS_00111591	P9	-
TCONS_00083148	P4	-
TCONS_00140595;TCONS_00140597;TCONS_00140603	P9;P8	-
TCONS_00108714	P12	-
TCONS_00095744	P9	-
TCONS_00018508	P1	-
TCONS_00053148	P8	-
TCONS_00253003	P5	-
TCONS_00113462	P8	-
TCONS_00110665	P9	-
TCONS_00112218	P9	-
TCONS_00117137	P9	-
TCONS_00107451	P10	-
TCONS_00111593;TCONS_00111597	P13;P9	-
TCONS_00107534	P9	-
TCONS_00197324	P12	-
TCONS_00107416	P11	-
TCONS_00107411	P10	-
TCONS_00111603	P11	-